# First insights into lichen symbiont associations along a successional gradient in the glacier forefield of Ödenwinkelkees (Hohe Tauern, Austria)

Sven Gindorf[1], Ulrike Ruprecht[1*]

Although lichens play a central role in primary succession, they have so far been largely overlooked in ecological research on glacier forefields. This study presents the first molecular assessment to investigate association patterns of dominant lichen symbionts along a succession gradient in the glacier forefield of the Ödenwinkelkees (Hohe Tauern, Austria).

In a pilot study, lichen diversity and coverage was assessed across 11 permanently marked 1×1 m plots of the Ödenwinkel Research Platform, spanning ~225 years of deglaciation. Dominant lichen symbionts (mycobiont [fungus], photobiont [algae]) were molecularly identified using the classic barcode marker ITS and lichen cover was quantified from rectified top-view images. Assembly- and community patterns were explored using network- and multivariate statistics. A hump-shaped pattern of species richness was observed, peaking at ~100 years since deglaciation. Rock dwelling lichens dominated early stages, while soil dwelling species increased after ~46 years and prevailed at intermediate ages (mean coverage ~36%). Photobiont identity appeared to mediate mycobiont ecological range, with generalist fungi associating with multiple algal partners. Field assessable groups effectively indicated successional stage, and the mean thallus area of yellow *Rhizocarpon* spp. emerged as a promising proxy for terrain age.

This study highlights lichen community turnover and photobiont-mediated filtering along primary succession and provides a basis for future molecular and image-assisted lichenological research in alpine environments.

**Gindorf S, Ruprecht U (2026) Erste Einblicke in die Assoziationsmuster der Symbiosepartner von Flechten entlang eines Sukzessionsgradienten im Gletschervorfeld des Ödenwinkelkees (Hohe Tauern, Österreich)**

Obwohl Flechten eine zentrale Rolle in der Primärsukzession einnehmen, werden sie in der ökologischen Forschung zu Gletschervorfeldern bislang kaum berücksichtigt. Diese Studie präsentiert erstmals mit molekularen Methoden die Assoziationsmuster der dominanten Flechtensymbionten entlang eines Sukzessionsgradienten im Gletschervorfeld des Ödenwinkelkees (Hohe Tauern, Österreich).

In einer Pilotstudie wurden Flechtenvielfalt und -bedeckung auf 11 permanent markierten 1 × 1 m großen Parzellen der Research Platform Ödenwinkel untersucht, die ~225 Jahre seit der Entgletscherung abdecken. Die dominante Flechtensymbionten (Mykobiont [Pilz], Photobiont [Alge]) wurden mit Hilfe des klassischen Barcodemarker ITS molekular identifiziert und die Bedeckung wurde aus orthorektifizierten Bildaufnahmen quantifiziert. Gemeinschaftsmuster wurden mithilfe von Netzwerk- und multivariater Statistik analysiert.

Die Artenvielfalt folgte einem unimodalen Muster mit einem Höhepunkt etwa 100 Jahre nach der Entgletscherung. In frühen Stadien dominierten steinbewohnende Flechten, während bodenbewohnede Arten nach ~46 Jahren zunahmen und in mittleren Stadien vorherrschten (mittlere Bedeckung ~36 %). Die Identität des Photobionten schien das ökologische Spektrum des Mykobionten zu beeinflussen, wobei Generalisten mit mehreren Algenpartnern assoziiert waren. Feldbestimmbare ökologische Gruppen erwiesen sich als effektive Indikatoren für das Sukzessionsstadium, und die gemittelte Thallusfläche gelber *Rhizocarpon*-Arten zeigte Potenzial als Indikator des Moränenalters.

Diese Studie untersucht die Dynamik von Flechtengemeinschaften sowie die Assoziationen dominanter Symbiosepartner entlang eines Gradienten und liefert damit eine Grundlage für ein besseres Verständnis von Sukzessionsprozessen genauso wie für zukünftige molekulare und bildbasierte Untersuchungen.

**Keywords:** saxicolous lichens, terricolous lichens, successional gradient, chronosequence, lichen symbionts, photobiont guilds, glacier forefield, primary succession.

**Received:** 2025 09 09

**DOI:** https://doi.org/10.25365/azba.162.22

[1] Paris Lodron Universität Salzburg, Hellbrunnerstraße 34, 5020 Salzburg, Austria

* Corresponding author: ulrike.ruprecht@plus.ac.at

## Introduction

Accelerating climate change is causing the rapid melt of glaciers in the European Alps (Cannone et al. 2008; Roe et al. 2017). In glacier forefields, the retreating glacier tongue successively uncovers fresh terrestrial habitat that becomes available for de novo colonization by a wide range of taxa. This process creates a predictable gradient of environmental conditions along which primary succession unfolds, known as the successional gradient (Miller & Lane 2019), making glacier forefields excellent 'natural laboratories' to study ecosystem development and species assembly along chronosequences (Bradley et al. 2014; Junker et al. 2021;He et al. 2023).

Succession in glacier forefields typically follows a predictable pattern, which can be studied using a space-for-time substitution approach (Lovell et al. 2023). As distance from the glacier front increases, so does the age of the substrate, offering a proxy for temporal development. The community dynamics in glacier forefields are generally shaped by two main mechanisms: i) directional replacement of communities composed of only few pioneer species and ii) the directional accumulation of species along the successional gradient leading to a nested community structure (Nascimbene et al. 2017).

While the successional dynamics of vascular plants and many cryptogamic organisms in glacier forefields are relatively well studied (e.g. Faegri 1934; Favero-Longo et al. 2012; Erschbamer & Caccianiga 2016; Schumann et al. 2016; Junker et al. 2021), much less is known about the successional dynamics of lichens, particularly the interactions of their symbiotic partners along chronosequences. The symbiotic associations consist of heterotrophic fungi (mycobionts) and photosynthetic microalgae or cyanobacteria (photobionts). Most mycobionts belong to the Ascomycota, with a smaller fraction (~2%) to Basidiomycota (Lumbsch & Leavitt 2011). Approximately 85% of lichens associate with green algae, 10% with cyanobacteria, and 3–4% with both partners (Sanders & Masumoto 2021). Photobiont associations are often variable: one mycobiont may associate with different photobionts, sometimes even from distinct genera, depending on environmental context (Perez-Ortega et al. 2012; Wagner et al. 2021). These associations are also commonly structured in so-called photobiont-mediated guilds – groups of mycobionts ecologically connected through their use of the same photobiont pool (Rikkinen 2007; Duran-Nebreda & Valverde 2022).

Lichens are renowned pioneer organisms on newly exposed substrates (e.g. Türk & Erschbamer 2010; Favero-Longo et al. 2012; Wietrzyk-Pelka et al. 2018) contributing to stabilization, erosion resistance and fertilization in soil formation processes (Büdel & Colesie 2014; Ruprecht et al. 2014; Zavarzina et al. 2019). Despite their ecological relevance, lichens are often overlooked in successional studies, which traditionally emphasize vascular plants or microbial communities (e.g. Junker et al. 2021).

Many lichenological studies in glacier forefields have aimed to estimate moraine age using the thallus size of *Rhizocarpon* species with yellow thalli – commonly referred to as "yellow rhizocarpons" (e.g. Mottershead & White 1972; Proctor 1983; Garibotti & Villalba 2009; Loso et al. 2014). This approach, known as lichenometry, is based on the assumption that the largest thalli on surfaces of unknown age share comparable colonization histories, growth rates, and mortality dynamics with those on dated reference surfaces, allowing terrain age to be inferred after appropriate calibration (Armstrong 2016). However, the fundamental assumptions underlying lichenometry have long been debated. For instance, apparently large thalli may represent the coalescence of several individuals or may have been displaced by geomorphic processes such as rockfall, thereby challenging the reliability of size-based age estimates (Osborn et al. 2015). These limitations highlight the potential of alternative, statistically robust approaches to linking lichen growth patterns with moraine age, such as analyses based on mean thallus size rather than single largest individuals.

The comparatively few studies focusing on lichen diversity in glacier forefields have primarily addressed the visible fungal component of the lichen thallus, with only limited attention given to photobiont identity and dynamics (e.g. Türk & Erschbamer 2010; Favero-Longo et al. 2012; Nascimbene et al. 2017;). Nevertheless, recent molecular approaches have begun to reveal patterns of symbiont turnover along environmental gradients. For example, Beck et al. (2019, 2023) demonstrated shifts in lichen symbiont associations along Antarctic chrono sequences, highlighting the ecological role of photobionts in shaping lichen community assembly. More broadly, the composition and turnover of mycobiont–photobiont associations can reflect environmental filtering and symbiotic specificity (Blaha et al. 2006; Dal Grande et al. 2018), and such turnover may follow predictable trajectories along environmental gradients (Rolshausen et al. 2020, 2023). Together, these findings suggest that generalist mycobionts may respond to environmental variability by associating with different photobionts across conditions, thereby expanding their ecological niche through an enlarged "mutualistic niche" (Peay 2016).

In glacier forefields, Favero-Longo et al. (2012) described three major stages of cryptogam succession: pioneer assemblages within decades, intermediate stages after ~30–40 years, and a climax stage in the oldest terrain. These shifts often reflect increasing habitat stability and resource availability. While the pioneer assemblages consist mainly of saxicolous (rock dwelling) lichens, terricolous (soil dwelling) lichens generally increase in abundance and coverage from the intermediate stages following a general trend of increasing lichen species richness with time of deglaciation associated with changes in community structure (Türk & Erschbamer 2010; Favero-Longo et al. 2012; Nascimbene et al. 2017; Wietrzyk-Pelka et al. 2018).

Although molecular techniques such as ITS sequencing have revealed cryptic diversity among dominant symbiotic partners in lichens and challenged classical views of the specificity of mycobionts to their photobionts along climate gradients (Nelsen & Gargas 2009; Kraichak et al. 2015, Muggia et al. 2018; Ruprecht et al. 2020, Wagner et al. 2021) no studies have so far applied molecular tools for lichenological studies in glacier forefields. Traditional morphological identification of lichen symbionts – especially of crustose lichens from families such as Lecideaceae – is notoriously difficult due to their reduced

and often convergent phenotypic traits (Ruprecht et al. 2020). As a result, the use of molecular tools has become indispensable for accurate species delimitation in lichenological research (Bickford et al. 2007; Lumbsch & Leavitt 2011). DNA-based methods – such as probabilistic phylogenetic reconstruction or DNA barcoding using ITS markers – allow for reliable identification of both mycobionts and photobionts, even in morphologically cryptic taxa (Ruprecht et al. 2020). The ITS region has emerged as the most robust universal barcode for myco- (Yahr et al. 2016) as well as photobiont (Ruprecht et al. 2014; Muggia et al. 2020) identification. These approaches are especially critical in ecological settings like glacier forefields, where many lichen individuals are early-successional pioneers with underdeveloped, cryptic morphology and potentially dynamic symbiotic associations. By applying molecular techniques to both symbiotic partners, it becomes possible to uncover fine-scale patterns of biodiversity, community turnover, and specificity that remain hidden to morphology-based approaches alone.

In this study, we investigated the diversity, distribution and coverage of lichens along a well-defined successional gradient in the glacier forefield of the Ödenwinkelkees (Hohe Tauern National Park, Austria). We investigated 11 representative plots along the gradient (2008–1797 years) of the Research Platform Ödenwinkel, which comprises 140 permanent plots along the chronosequence and offers extensive ecological and environmental data for comparison (Junker et al. 2020), by assessing (1) the diversity of dominant lichen symbionts in the glacier forefield, (2) the associations of dominant symbiotic partners at different successional stages using network statistics and (3) the relationship between moraine age and mean thalli size of yellow *Rhizocarpon* individuals.

## Material and Methods

### Study area and investigated lichen specimens

A total of 94 lichen samples (69 saxicolous, 25 terricolous) were collected along the chronosequence of the Ödenwinkelkees glacier forefield (Hohe Tauern National Park, Austria; Electronic Supplement Fig. S1). Eleven 1×1 m plots from the Research Platform Ödenwinkel (Junker et al. 2020) were selected to represent distinct moraine ages and grouped into successional stages (Fig. 1; Appendix Tab. A1).

Lichen diversity was pre-assessed morphologically on site. In order not to disturb the species composition in the plots, only one sample/species was collected per plot (duplicates excluded post-hoc) by using sterile scalpels or forceps and stored in labelled tubes for molecular analyses. We were not able to collect herbarium vouchers for our molecular samples because the plots were part of a long term ecological observation study and the physical conditions were supposed to be left as unaltered as possible. We prioritized the advantage of the inventory for comparison of Research Platform Ödenwinkel over reproducibility. With reference to the plot and top view image, the studied lichen thalli can be assessed on site.

Top-view plot photographs were taken using a handheld DSLR camera (Sony Alpha 77; Electronic Supplement Fig. S1).

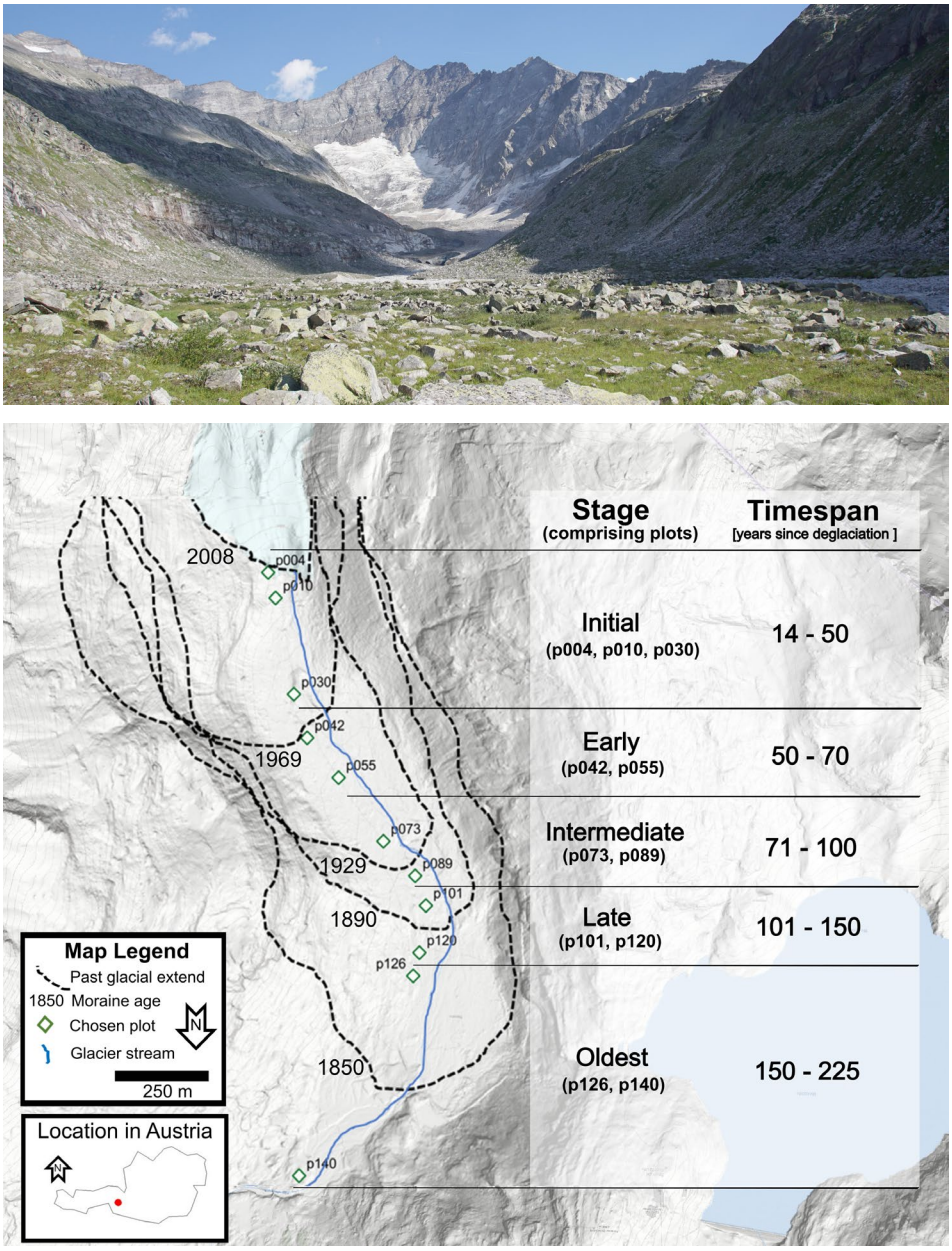


**Fig. 1:** Chosen plots of the Research Platform Ödenwinkel (Junker et al., 2020) with location in Austria, past glacier extent, and successional stages assigned in this study. The map was created using QGIS (v.3.16; and is based on basemap layers of Austrian administrations (www.basemap.at). | **Abb. 1:** Ausgewählte Parzellen der Forschungsplattform Ödenwinkel (Junker et al., 2020) in Österreich, ehemaligem Gletscherausmaß und in dieser Studie verwendeten Sukzessionsstadien. Die Karte wurde mit QGIS (v.3.16; www.qgis.org) erstellt und basiert auf Basiskartenebenen österreichischer Behörden (www.basemap.at).

## Molecular Analyses

Total genomic DNA was extracted from small thallus fragments using the DNeasy Plant Mini Kit (Qiagen), followed by further purification with the ZymoBIOMICS DNA Miniprep Kit (Zymo Research), following the manufacturers' protocols with minor modifications (Ruprecht et al. 2020). For amplification of the internal transcribed spacer (ITS) region of the nuclear ribosomal DNA, taxon-specific primer pairs were used:

**Mycobiont.** ITS1F and ITS4 (Gardes & Bruns 1993; White et al. 1990) were used with standard conditions (Ruprecht et al. 2020). Failed reactions were repeated using a semi-nested PCR with ITS1 and ITS4 (White et al. 1990).

**Photobiont.** To assess the presence of different green microalgae associated to the mycobiont, a broad screening along the ITS region was performed using the different primers pairs ITS4T and ITS1T (Kroken & Taylor 2000), ITS4 and nr-SSU-1780-5' (White et al. 1990; Piercey-Normore & DePriest 2001;) as well as ITS2-antisense A and ITS1-sense A (Ruprecht et al. 2014) as described in Ruprecht et al. (2020).

Unpurifed PCR products were sent to Eurofins Genomics (Germany) for Sanger sequencing.

## Species delimitation

Sequences were edited and aligned using the software Geneious (v.6.1.8.; http://www.geneious.com) MAFFT v7.017 (Katoh et al.2002).

Since we were not allowed to collect herbarium specimens in order to minimize disturbance to the habitat, we identified the samples using a BLAST search (www.blast.ncbi.nlm.nih.gov) for all accessions and included both blast search results and own sequences in comparative ML trees for the mycobionts. Since our own sequences were available, the samples from the family Lecideaceae were added to the existing phylogeny from Ruprecht et al. 2020 (SI 2) in order to assign them more accurately. For all the other sequences we downloaded matching sequences and combined them with the samples of the study in a Maximum Likelihood analysis using the IQ-TREE web server with default settings (Nguyen et al. 2015) to define the different species groups (SI 3). Tree visualization was performed with FigTree v1.4.4 (Rambaut 2018). The photobionts were solely assigned via BLAST search, the identity values were shown directly in Appendix Tab. A2.

Additionally, taxonomic assignments of mycobionts were based on alignment with field photos. Top-view plot photographs were taken using a handheld DSLR camera (Sony Alpha 77; Electronic Supplement Fig. S1).

## Image-based coverage analysis

Top-view photographs of the plots were rectified in R (R Core Team 2022) using the packages devtools (Wickham et al. 2022), gplots (Warnes et al. 2016), and gdalUtilities (O'Brien 2019). Spatial analysis of surface coverage was conducted in QGIS v.3.16 using the coordinate reference system WGS84 / Pseudo-Mercator (EPSG:3857). Polygons were

manually delineated at multiple magnification levels to classify surface types. The area of each polygon was then calculated automatically by the software, allowing percentage cover of each surface class to be derived.

The following cover classes were distinguished:

- Vegetation (vascular plants and mosses)
- Rock (coarse substrate, Ø > 63 mm)
- Soil (fine substrate, Ø < 63 mm, without visible biological growth)
- Terricolous lichens
- Saxicolous lichens

In addition, the total surface area of *Rhizocarpon* spp. characterized by yellow-coloured thalli (hereafter referred to as yellow *Rhizocarpon*) was separately delineated and quantified.

## Statistical analyses

To explore lichen community dynamics along the successional gradient, we conducted a series of univariate and multivariate analyses using R (R Core Team 2022).

**Yellow rhizocarpons.** The dataset was corrected for outliers in thallus size separately for early (<70 years) and late (>70 years) successional stages based on interquartile range criteria. Log-transformation was applied to normalize the data. Group differences were tested using analysis of variance (ANOVA) followed by a Tukey HSD post hoc test. Assumptions of homoscedasticity and normality were assessed by visual inspection of model residuals. Group-level means and standard deviations were calculated to visualize trends across the chronosequence. For correlation analyses, Spearman's rank correlation was used.

**Multivariate analyses:** For all multivariate analyses, the package vegan in R (Oksanen et al. 2013) was applied.

**Non-metric multidimensional scaling (NMDS)** was applied to a presence/absence species matrix (Euclidean distance, k = 2) and ordihulls were drawn depicting rock coverage (<30% vs. >30%) and species richness (<6 vs. >6).

**Principal Component Analysis (PCA)** was performed on raw coverage data (area in $mm^2$) combined with environmental variables from Junker et al. (2020), including soil temperature, pH, and concentrations of nitrogen (N), phosphorus (P), magnesium (Mg), and potassium (K), as well as substrate age. Variables were standardized prior to analysis.

**Redundancy Analysis (RDA)** was used to assess relationships between lichen species composition and environmental conditions. The species matrix was the same as in NMDS and

the environmental matrix included the raw coverage data used for the PCA. Significance was tested with 999 permutations.

## Ecological assignment

To identify meaningful patterns in symbiotic associations and to reduce noise caused by single-species occurrences, both myco- and photobionts were grouped into ecologically and functionally coherent categories. The classification followed a stepwise decision scheme based on the ecological and morphological traits of the lichen-forming fungi (Tab. 1):

- **Substrate Affinity:** First, species were divided by substrate: terricolous vs. saxicolous. Substrate type is one of the most consistent ecological filters along glacier forefield chronosequences.
- **Genus-Level Identity:** Species were then grouped at the genus level when multiple representatives of a genus occurred in the dataset. This allowed grouping of functionally or ecologically similar species.
- **Family-Level Identity:** In cases where genus-level resolution was not sufficient (e.g. crustose lichens with reduced morphology), species were grouped at the family level, particularly within Lecideaceae, which includes morphologically difficult to assign taxa such as *Lecidea* and *Porpidia*.

**Tab. 1:** Ecological groupings of mycobiont taxa based on a stepwise classification scheme. | **Tab. 1:** Ökologische Gruppierungen von Mykobionten-Taxa auf der Grundlage eines schrittweisen Klassifizierungsschemas.

| Group | Grouping scheme |
|---|---|
| stereocaulon_soil | 1. Substrate: terricolous; 2. Genus: *Stereocaulon* sp. |
| stereocaulon_rock | 1. Substrate: saxicolous; 2. Genus: *Stereocaulon* sp. |
| aspicilia | 1. Substrate: saxicolous; 2. Genus: *Aspicilia* sp. |
| bellemerea | 1. Substrate: saxicolous; 2. Genus: *Bellemerea* sp. |
| cetraria | 1. Substrate: terricolous; 2. Genus: *Cetraria* sp. |
| lecanora | 1. Substrate: saxicolous; 2. Genus: *Lecanora* sp. |
| rhizocarpon | 1. Substrate: saxicolous; 2. Genus: *Rhizocarpon* sp. |
| umbilicaria | 1. Substrate: saxicolous; 2. Genus: *Umbilicaria* sp. |
| lecideaceae | 1. Substrate: saxicolous; 2. Genus: *Lecidea* sp. & *Porpidia* sp.; 3. Family: Lecideaceae |
| cladonia_r | 1. Substrate: terricolous; 2. Genus: *Cladonia* sp.; 3. Family: Cladoniaceae; 4. "Reindeer lichens" with extensively branched morphology |
| cladonia_s | 1. Substrate: terricolous; 2. Genus: *Cladonia* sp.; 3. Family: Cladoniaceae; 4. Shrubby morphology with podetia |

- **Functional Morphology:** Finally, functional or growth-form traits were used to refine groupings, particularly for morphologically diverse genera like *Cladonia* P.Browne (e.g. differentiating extensively branched "reindeer lichens" from shrubby podetia-forming species).

*Asterochloris* and *Trebouxia* Photobionts were grouped accordingly. All other photobionts were grouped as OGEM ("Other Green Eukaryotic Microalgae"). This classification aimed to reflect ecological strategies relevant to succession, rather than strict phylogenetic relationships.

# Results

## Species delimitation

Species-level identification was successfully obtained for 84 mycobionts and 72 photobionts.

**Mycobionts:** Among the taxonomically challenging groups, five distinct clades were identified within Lecideaceae (*Lecidea promiscens* Nyl., *Lecidea* sp., *L. plana* (J. Lahm) Nyl, *Porpidia macrocarpa* (DC.) Hertel & A.J.Schwab, and *Lecidea* sp. UR01405*)*. All other specimens were assigned to species level via BLAST search to the genera *Cladonia*, *Rhizocarpon* Ramond ex DC., *Stereocaulon* Hoffm., *Bellemerea* Hafellner & Cl.Roux, *Lecanora* Ach., *Umbilicaria* Hoffman, *Aspicilia* A.Massal., and *Cetraria* Ach.

**Photobionts:** *6 species were assigned to the genus Asterochloris* including *A. glomerata* (Warén) Skaloud & Peksa, *A. irregularis* (Hildreth & Ahmadijan) Skaloud & Peksa, A. *lobophora* (Skaloud & Peksa 2015), A. *stereocaulonicola* Y.J.Kim, J.I.Kim & W.Shin and the OTUs *A.* sp. Vancourova A588, *A.* sp. 2709. The *Trebouxia* sequences formed two major clusters corresponding to OTUs *Trebouxia* (*Tr*_I01) and *T.* (*Tr*_S02) (Muggia et al. 2020)

Full species assignments are listed in Appendix Tab. A2, phylogenetic trees are provided in Electronic Supplement Figs S2–S3.

## Species assessment and grouping

From 84 successfully sequenced mycobionts, 64 unique occurrences (one species per plot) were retained, comprising 42 saxicolous and 23 terricolous taxa. Species richness varied across plots and generally peaked (10 species) in mid-successional stages (Fig. 2), while the youngest and oldest plots exhibited lowest species richness (p004: 1 species; p010: 2 species; p140: 3 species).

**Mycobionts.** In total, 30 mycobiont species from 10 genera were identified and grouped into 11 ecologically coherent categories based on substrate affinity, morphology, and taxonomy (Fig. 3). The most widespread species were *Lecidea promiscens* and *Rhizocarpon geographicum* (L.) DC., each found on 8 plots. *Stereocaulon alpinum* Laurer and *Lecanora polytropa* (Hoffm.) Rabenh. were observed on 5 plots. *Bellemerea* sp. and *Rhizocarpon polycarpum (Hepp ex Arnold)* Th.Fr. were found on 4 plots. *Stereocaulon nanodes* Tuck occurred on 3 plots, one specimen growing on rock and the others on soil. One species only occurred

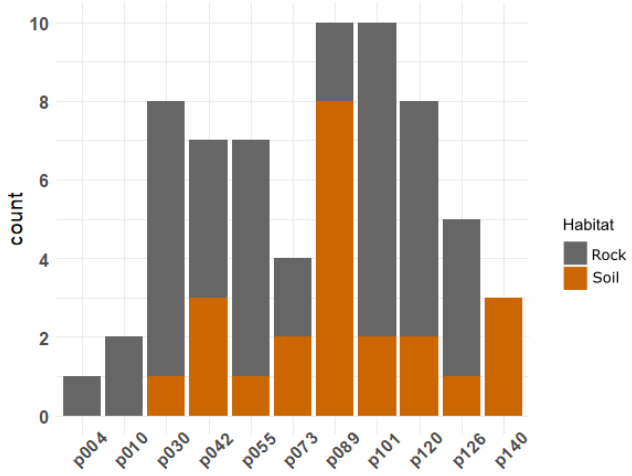


**Fig. 2:** Species richness and habitat distribution across plots. Bar plots showing the number of unique lichen species per plot highlighting shifts in richness and substrate preference along the successional gradient. | **Abb. 2:** Artenreichtum und Lebensraumverteilung über die Parzellen hinweg. Balkendiagramme zeigen die Anzahl der verschiedenen Flechtenarten pro Parzelle und verdeutlichen Veränderungen im Artenreichtum und in der Substratpräferenz entlang des Sukzessionsgradienten.

on a single plot, such as *Lecidea plana* (J. Lahm) Nyl.. The heterogeneous genus *Cladonia* P. Browne exhibited the highest number of different species (n=11).

**Photobionts.** 64 sequences revealed 11 distinct taxa: 6 species of the genera *Asterochloris*, two OTUs of *Trebouxia*, and one each of *Chloroidium* Nadson, *Pseudochlorella* J.W.G.Lund, 1955 and an 'uncultured algal isolate'. The most common photobionts were *Tr*_I01 and *Tr*_S02, primarily associated with saxicolous mycobionts, while *Asterochloris glomerata* and *A. irregularis* were more frequently linked to terricolous partners (Fig. 4).

## Myco–photobiont network structure

Bipartite networks were calculated for all observed associations between mycobiont species and their respective photobiont taxa (Fig. 5). The overall network showed an intermediate specialization with an $H_2'$ value of 0.53. While some mycobionts (e.g. *Aspicilia* spp., *Umbilicaria* spp.) were associated exclusively with a single photobiont, others – such as *Stereocaulon alpinum*, *Lecidea promiscens*, and *Rhizocarpon polycarpum* – were associated with multiple photobionts, including different genera.

Additionally, bipartite networks were calculated for five successional stages (Fig. 6). The highest $H_2'$ value was observed in the late stage ($H_2'$= 0.80: highly specialized), followed by the initial stage ($H_2'$= 0.59). The young ($H_2'$= 0.14) and intermediate ($H_2'$= 0.24: highly generalized) stages showed lower specialization, while the oldest stage exhibited no network-level specialization ($H_2'$= 0.00). Shifts in photobiont associations were observed for different mycobionts, including *Lecidea promiscens* and *Rhizocarpon polycarpum*,

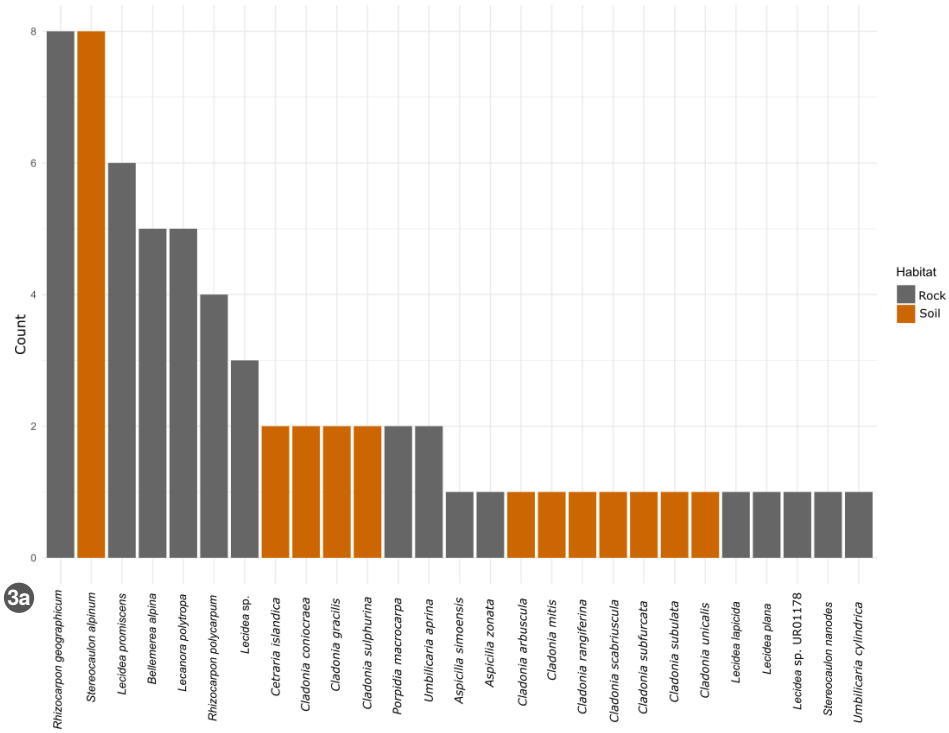
Count
0
2
4
6
8
Habitat
Rock
Soil
Rhizocarpon geographicum
Stereocaulon alpinum
Lecidea promiscens
Bellemerea alpina
Lecanora polytropa
Rhizocarpon polycarpum
Lecidea sp.
Cetraria islandica
Cladonia coniocraea
Cladonia gracilis
Cladonia sulphurina
Porpidia macrocarpa
Umbilicaria aprina
Aspicilia simoensis
Aspicilia zonata
Cladonia arbuscula
Cladonia mitis
Cladonia rangiferina
Cladonia scabriuscula
Cladonia subfurcata
Cladonia subulata
Cladonia unicalis
Lecidea lapicida
Lecidea plana
Lecidea sp. UR01178
Stereocaulon nanodes
Umbilicaria cylindrica

3a

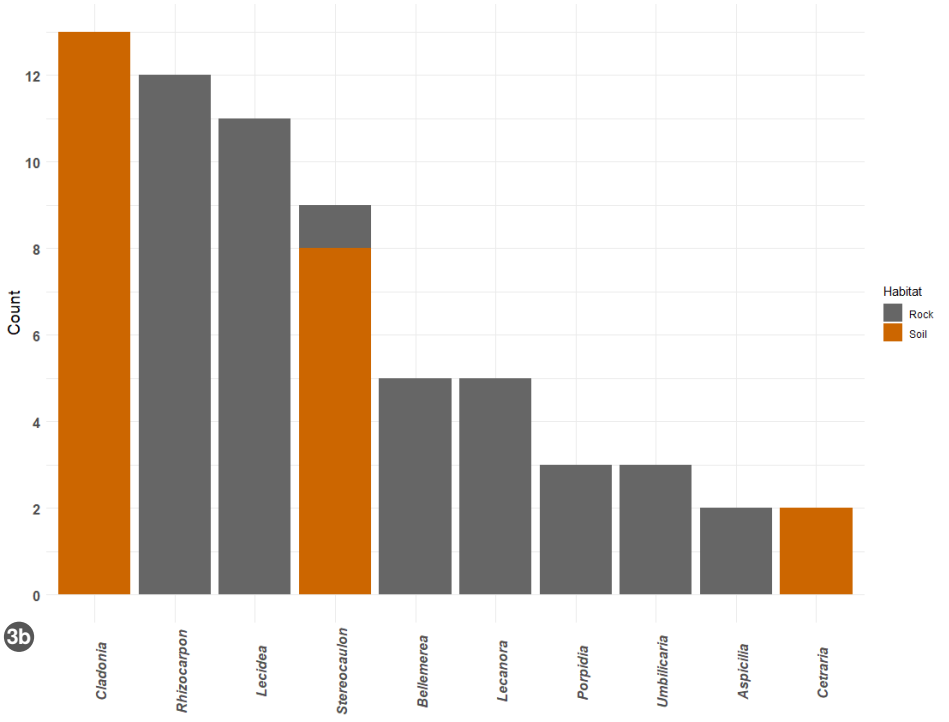
Count
0
2
4
6
8
10
12
Habitat
Rock
Soil
Cladonia
Rhizocarpon
Lecidea
Stereocaulon
Bellemerea
Lecanora
Porpidia
Umbilicaria
Aspicilia
Cetraria

3b

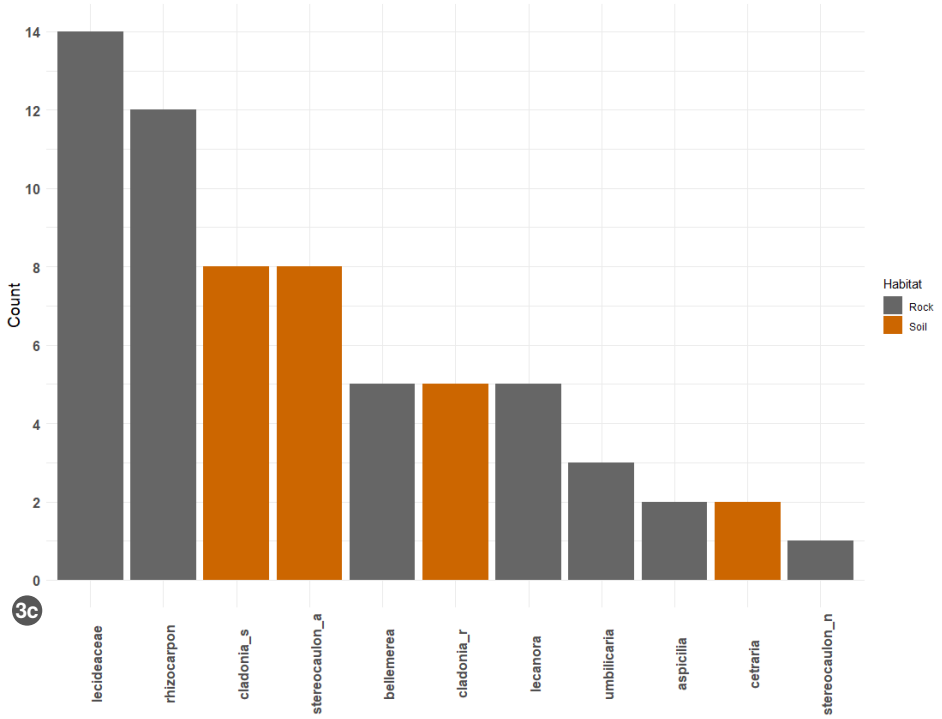


**Fig. 3:** Bar plots showing species richness of lichen taxa identified in this study. (a) species-level occurrences across plots, (b) distribution across genera, (c) grouping ecological categories. | **Abb. 3:** Balkendiagramme zur Artenvielfalt der in dieser Studie identifizierten Flechten-Taxa. (a) Vorkommen auf Artenebene in den verschiedenen Parzellen, (b) Verteilung über die Gattungen, (c) Einteilung in ökologische Kategorien.

indicating variable symbiotic patterns across successional stages. The two *Trebouxia* OTUs observed in this study were the most frequently associated photobionts and occurred across all stages. While the *Trebouxia* OTUs were dominant in the initial, young, and late stages, *Asterochloris* taxa prevailed in the intermediate stage: Despite *A. glomerata* occurring in almost all stages, they showed most associations to terricolous mycobionts in the intermediate stage. *A. irregularis* and *A. stereocaulonicola* occurred exclusively in this stage and exhibited an association to four different mycobiont taxa (including saxicolous *Porpidia macrocarpa*).

Across the successional gradient, *Sterocaulon alpinum* was the only mycobiont species observed in all five stages and associated with up to three different photobiont taxa. In contrast *S. nanodes* occurred only in the initial and late stage. Notably, OGEM-photobionts were only observed in two stages: *Chloroidium saccharophilum* (W.Krüger) Darienko et al. in the initial stage, and *Pseudochlorella pyrenoidosa* as well as an 'unknown algal isolate' in the late stage.

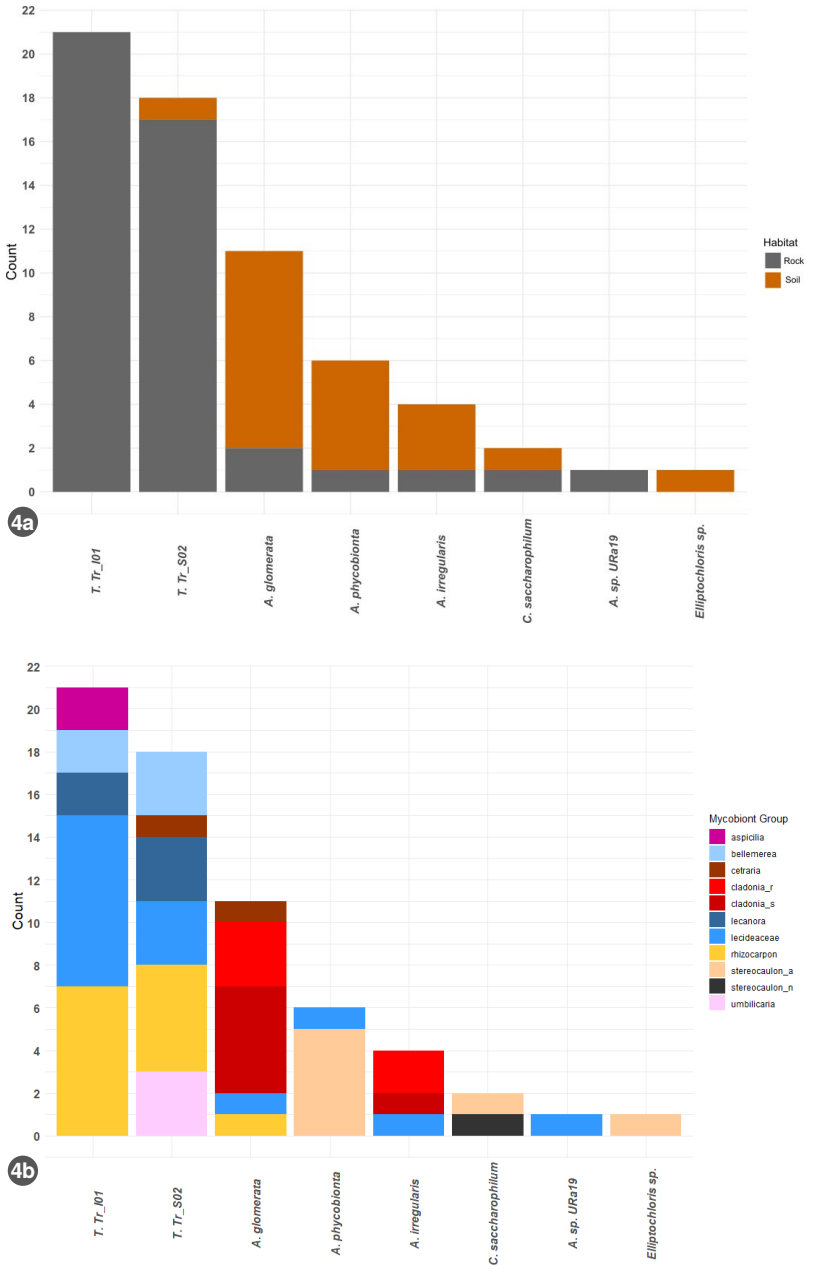


**Fig. 4:** Bar plots showing the occurrence of photobiont taxa (n = 64) across all lichen samples. (a) Distribution by substrate of the associated mycobiont (saxicolous vs. terricolous). (b) Associations of photobionts with ecologically defined mycobiont groups. | **Abb. 4:** Balkendiagramme, die das Vorkommen von Photobionten-Taxa (n = 64) in allen Flechtenproben zeigen. (a) Verteilung nach Substrat der assoziierten Mykobionten (saxikol vs. terrikol). (b) Assoziationen von Photobionten mit ökologisch definierten Mykobionten-Gruppen.

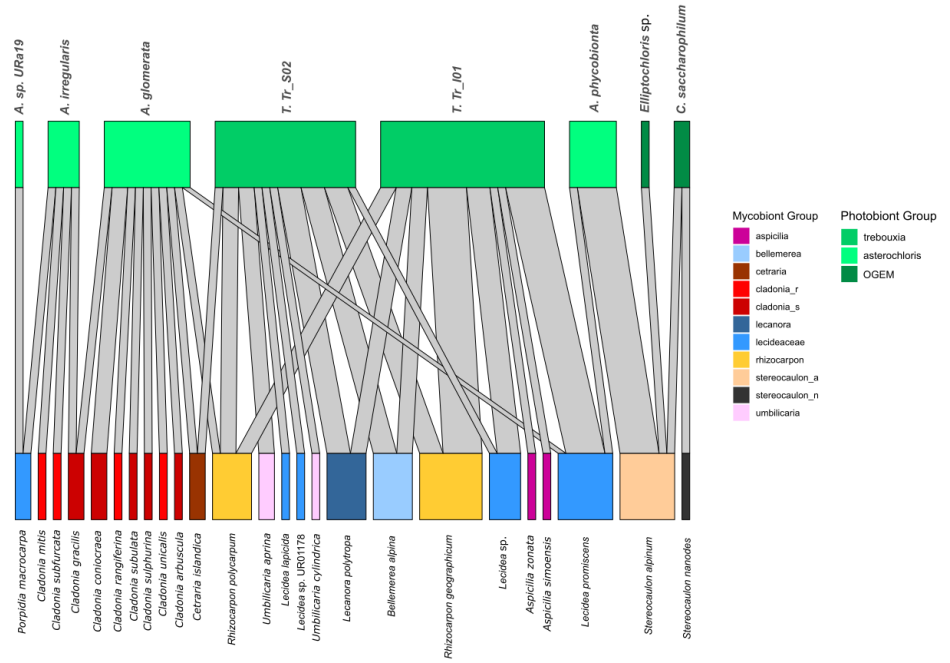


**Fig. 5:** Bipartite network of all observed mycobiont–photobiont associations ($H_2' = 0.52$). Mycobionts (lower level) and photobionts (upper level) are coloured by ecological group. Edge width indicates interaction frequency. | **Abb. 5:** Bipartites Netzwerk aller beobachteten Mykobionten-Photobionten-Assoziationen ($H_2' = 0{,}52$). Mykobionten (untere Ebene) und Photobionten (obere Ebene) sind nach ökologischen Gruppen farblich gekennzeichnet. Die Breite der Verbindungsbalken gibt die Häufigkeit der Interaktionen an.

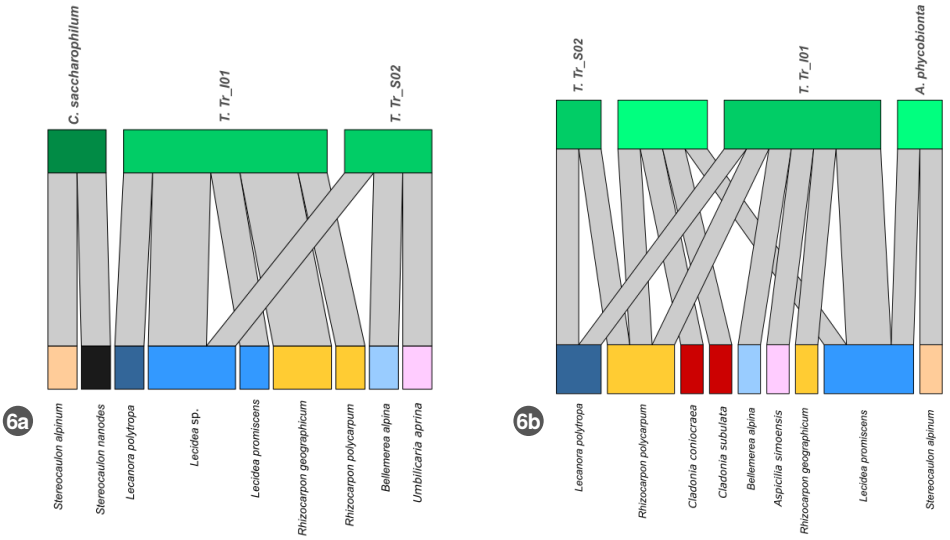

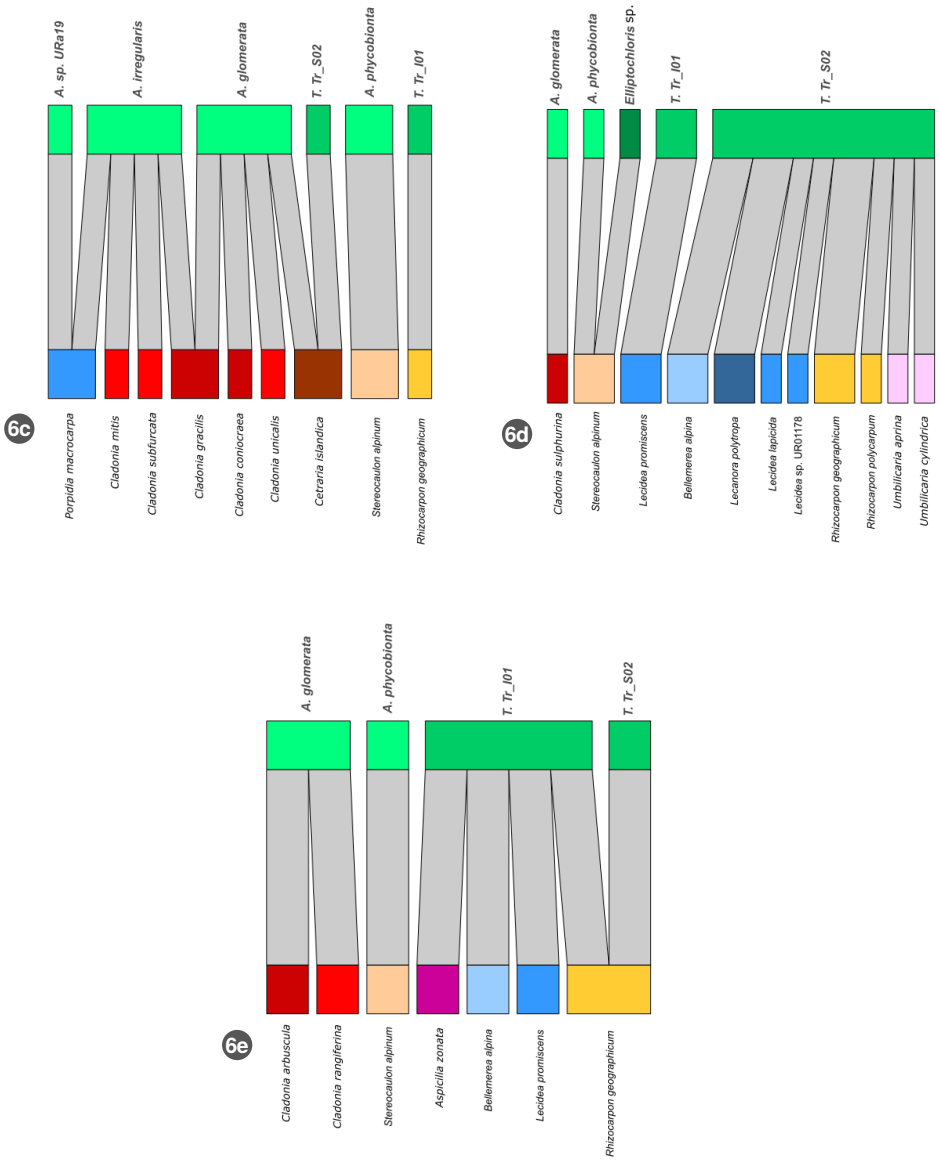


**Fig. 6:** Stage-specific bipartite networks of mycobiont–photobiont associations across five successional stages. (a) Initial (p004, p010), (b) Young (p042, p055), (c) Intermediate (p073, p089), (d) Late (p101, p120), (e) Oldest (p126, p140). Colours denote ecological groupings (colour code according to Fig. 5). Edge width indicates interaction frequency. | **Abb. 6:** Stadiumspezifische bipartite Netzwerke von Mykobiont-Photobiont-Assoziationen über fünf Sukzessionsstadien hinweg. (a) Anfangsstadium (p004, p010), (b) Jungstadium (p042, p055), (c) Zwischenstadium (p073, p089), (d) Spätes (p101, p120), (e) Ältestes (p126, p140). Farben kennzeichnen ökologische Gruppierungen (Farbcode gemäß Abb. 5). Die Breite der Verbindungsbalken gibt die Häufigkeit der Interaktionen an.

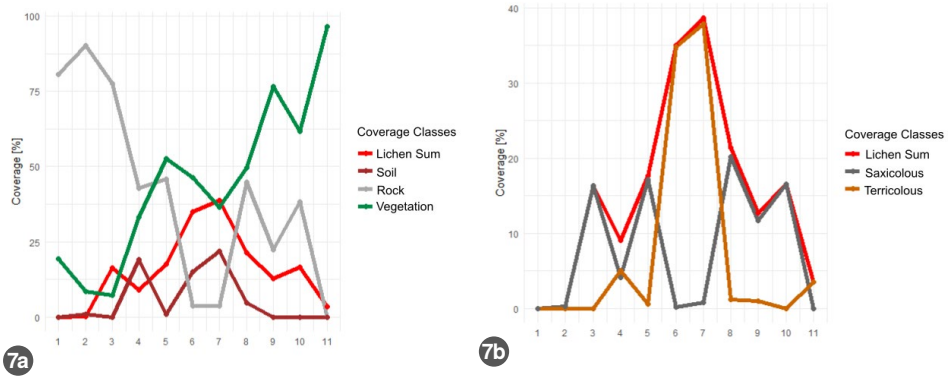


**Fig. 7:** Coverage trends of different substrate and lichen classes along the successional gradient. (a) Vegetation, soil, rock and total lichen cover; (b) Total lichen cover separated into terricolous and saxicolous growth forms. | **Abb. 7:** Bedeckungstrends verschiedener Substrat- und Flechtenklassen entlang des Sukzessionsgradienten. (a) Vegetations-, Boden-, Gesteins- und Gesamtflechtenbedeckung; (b) Gesamtflechtenbedeckung unterteilt in terrikole und saxikole Wuchsformen.

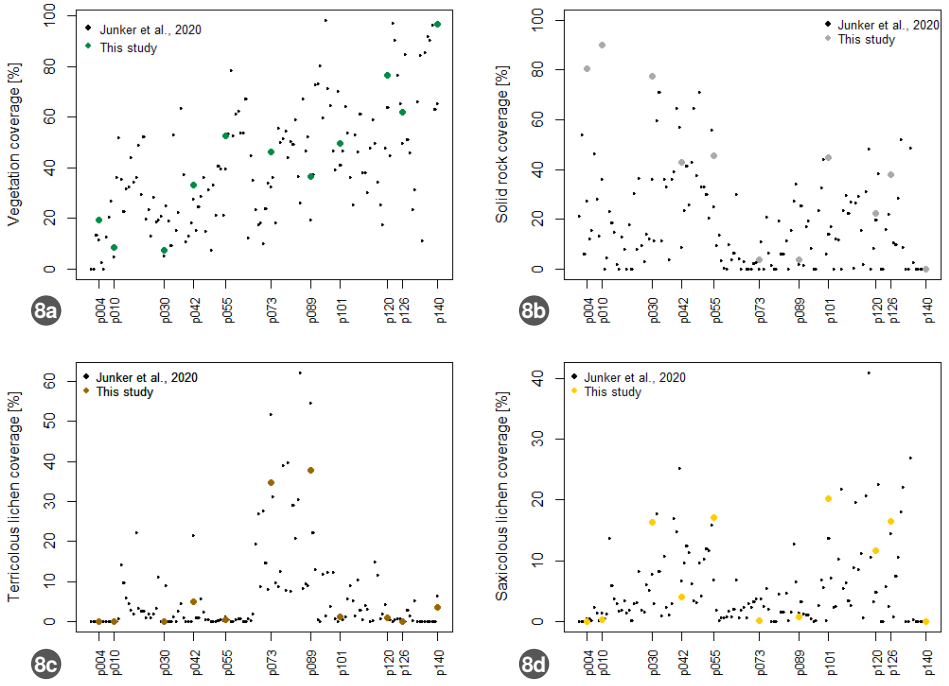


**Fig. 8:** Comparison of photo-based coverage data from this study (coloured dots) with field-based data of all 140 plots from Junker et al. (2020) (black dots) across all plots. (a) Vegetation, (b) solid rock, (c) terricolous lichens, (d) saxicolous lichens. | **Abb. 8:** Vergleich der fotobasierten Abdeckungsdaten aus dieser Studie (farbige Punkte) mit den Felddaten aller 140 Parzellen aus Junker et al. (2020) (schwarze Punkte) über alle Parzellen hinweg. (a) Vegetation, (b) festes Gestein, (c) terrikole Flechten, (d) saxikole Flechten.

## Coverage patterns along succession

Coverage estimates from photo-assessment reveal clear trends along the successional gradient (Fig. 7; Electronic *Supplement Fig. S1*). Vegetation cover increased to >95% with plot age ($R^2$ = 0.70), while rock cover declined from ~80% on the youngest plots to 0% on the oldest (Fig. 7a). Lichen cover peaked on intermediately aged plots (~39%) and was minimal at both early and late successional stages (Fig. 7b). This mid-successional peak was largely driven by terricolous lichens, particularly *Stereocaulon alpinum (*Electronic *Supplement Fig. S1).*

A comparison with field-assessed data by Junker et al. (2020) (Fig. 8a-d) confirms the general trends. Vegetation and lichen patterns broadly agree between studies, however, vegetation increase was steeper in our data and Junker et al. 2020 assessed terricolous lichen coverage of intermediate plots up to >60%. Rock cover estimates diverged slightly, with Junker et al. 2020 reporting lower values in the youngest stages, though both datasets showed a sharp decline towards intermediate plots.

### Yellow *Rhizocarpon* thallus area

The coverage data revealed a significant linear increase in mean thallus area of yellow *Rhizocarpon* specimens with age of deglaciation (LM: Df = 5, F = 54.08, p < 0.01; Fig. 9a). The differences in thallus size between plots were statistically confirmed via ANOVA followed by a Tukey-HSD post-hoc test (Fig. 9b). The latest successional plot with *yellow Rhizocarpon* presence (p126) exhibited significantly larger thalli than all others.

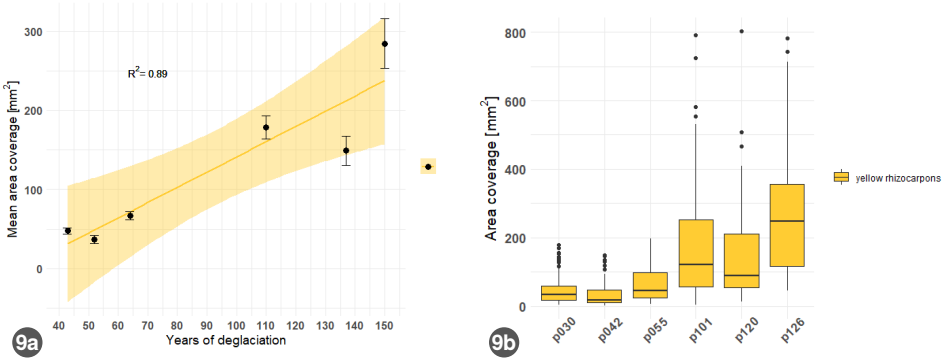


**Fig. 9:** (a) Linear regressions showing strong positive correlation ($R^2$ = 0.89) between mean yellow *Rhizocarpon* thallus size and plot age (obtained from Junker et al. 2020); (b) Thallus areas of yellow *Rhizocarpon* individuals across plots ordered by age. Lowercase letters indicate statistical groupings (Tukey HSD, p < 0.05). | **Abb. 9:** (a) Lineare Regressionen, die eine starke positive Korrelation ($R^2$ = 0,89) zwischen der durchschnittlichen Größe des Thallus von gelbem *Rhizocarpon* und dem Alter der Parzelle zeigen (entnommen aus Junker et al. 2020); (b) Thallusflächen von gelbem *Rhizocarpon*-Individuen über Parzellen hinweg, geordnet nach Alter. Kleinbuchstaben kennzeichnen statistische Gruppierungen (Tukey HSD, p < 0,05).

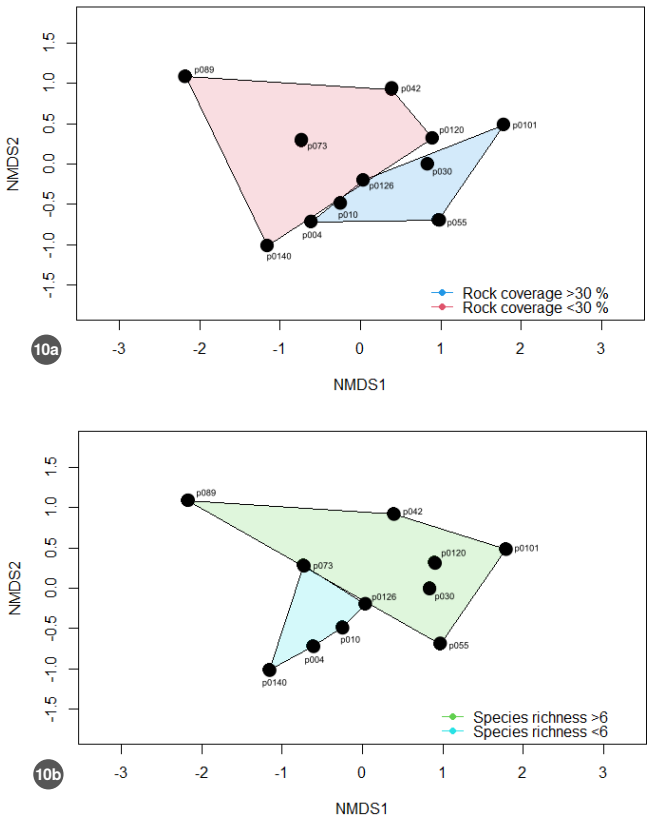


**Fig. 10:** NMDS ordination with plots grouped by (a) rock coverage (>30% vs. <30%) and (b) species richness (>6 vs. <6 species). | **Abb. 10:** NMDS-Ordination mit Parzellen gruppiert nach (a) Gesteinsbedeckung (>30 % vs. <30 %) und (b) Artenreichtum (>6 vs. <6 Arten).

## Multivariate analyses

Community structure was summarized using a two-dimensional NMDS (stress = 0.12). The NMDS1 axis tends to reflect rock coverage with a trend of terricolous-dominated communities (low rock cover) clustering at lower scores and saxicolous-dominated communities (high rock cover) at higher scores (Fig. 10a). NMDS2 tends to reflect a gradient in species richness, with species-poor plots (youngest and oldest) clustering at lower NMDS2 values and species-rich plots (intermediate ages) higher up (Fig. 10b). This separation by species richness was statistically supported (PERMANOVA: $F = 2.47$, $p = 0.015$).

In a PCA that included physico-chemical data of Junker et al. (2020) the first two axes (76% variance) confirmed two key correlations: (1) vegetation cover, nutrients (N, P, K, Mg) and moraine age increase together and are negatively related to pH and rock cover; (2) soil and terricolous-lichen cover track mean annual temperature and are negatively related to saxicolous cover (Fig. 11). The PCA suggests main environmental characterizations

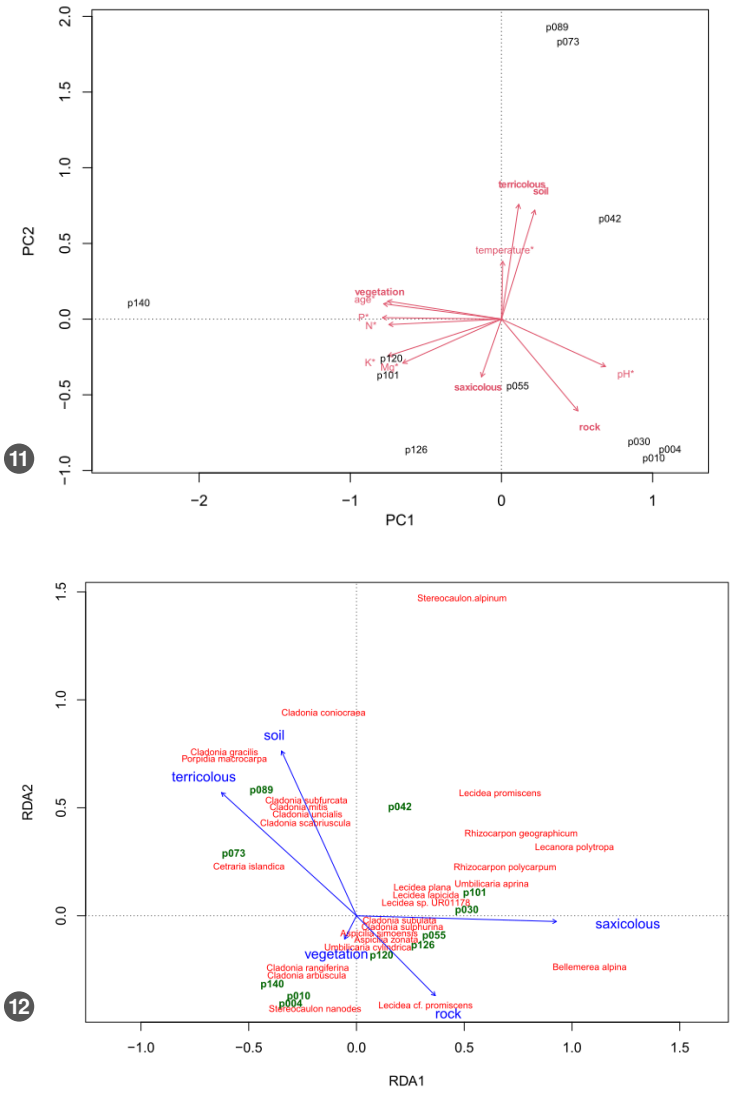


**Fig. 11:** Principal Component Analysis (PCA) of environmental and lichen coverage data. Coverage classes (bold) and environmental variables (asterisks) show distinct gradients along successional stages. The first two axes explain 76% of total variation. | **Abb. 11:** Hauptkomponentenanalyse (PCA) von Umwelt- und Flechtenbedeckungsdaten. Die Bedeckungsklassen (fett gedruckt) und Umweltvariablen (Sternchen) zeigen deutliche Gradienten entlang der Sukzessionsstadien. Die ersten beiden Achsen erklären 76 % der Gesamtvariation.

**Fig. 12:** Ordination plot of Redundancy Analysis (RDA) illustrating the effect of lichen coverage classes on species composition (F = 1.79, p = 0.007). Blue arrows represent coverage variables; red text indicates species scores. Plot IDs are represented in green. | **Abb. 12:** Ordination plot der Redundanzanalyse (RDA), der den Einfluss der Flechtenbedeckungsklassen auf die Artenzusammensetzung veranschaulicht (F = 1,79, p = 0,007). Blaue Pfeile stehen für Bedeckungsvariablen, roter Text gibt die Artenwerte an. Die Plot-IDs sind grün dargestellt.

of the plots: rock coverage and pH (p004, p010, p030), saxicolous lichen coverage (p055, p126), terricolous/ soil coverage and temperature (p089, p073), vegetation and nutrients (p101, p120, p140). One plot (p042) is found in the space between the axis of pH and soil coverage.

An RDA ordination plot links community composition with coverage data as constraining variables (Fig. 12). These variables explained 74.72% of the variance (global permutation test, F = 1.79, p = 0.007). The first axis reflects the terricolous–saxicolous trade-off, while the second axis separates species-rich intermediate plots from species-poor plots in the early and late stages. Plotting highest on RDA2 and intermediate at RDA1, *Stereocaulon alpinum* reflects high species richness and transition between rock and soil dominated areas. Characteristic taxa fall into the expected quadrants: Saxicolous mycobionts like *Lecidea* spp. and *Bellemerea* sp. align with rock/saxicolous coverage and terricolous species like *Cladonia* spp. or *Cetraria islandica* (L.) Ach. align with soil/terricolous coverage. The communities of the assessed plots show distinct clusters along the constraining axes: Youngest and oldest plots (p004, p010, p126) cluster below the vegetation axis. The plots p030, p055, p101, p120, p126 show a tendency of plotting around the rock- and saxicolous axis, while p073 and p089 form a cluster around the soil- and terricolous axis. Plot p042 is characterized by positive scores on both RDA axes and is associated with both saxicolous and soil explanatory variables.

## Discussion

### Species richness and community clusters

By combining molecular identification and community analyses, this pilot study uncovers new insights into successional trends and symbiotic turnover in lichen communities of the Ödenwinkelkees glacier forefield.

Saxicolous lichens outnumbered terricolous lichens nearly twofold, mirroring patterns reported in other glacier forefields (Türk & Erschbamer 2010; Favero-Longo et al. 2012). The number of terricolous species falls at the lower end of the range as reported in other glacier forefields by Nascimbene et al. (2017) (15 species at Morteratsch forefield, CH; 41 Gaisbergferner forefield, AT) or Wietrzyk-Pelka et al. (2018) (24 at Ferdinandbreen forefield, NO; 82 at Rieperbreen forefield, NO). In agreement with these studies, low species richness was observed on the youngest moraines. Colonization typically requires 30–40 years of deglaciation, as earlier substrates remain too unstable (Türk & Erschbamer 2010; Nascimbene et al. 2017). While other studies (Favero-Longo et al. 2012; Nascimbene et al. 2017; Wietrzyk-Pelka et al. 2018) reported positive succession–diversity relationships along the gradient, the present data suggests a hump-shaped pattern, with peak richness and coverage occurring in intermediately aged plots (~80–100 years; Fig. 1 & 2). Yet, a drop in species richness was observed after 83 years of deglaciation (p073; Fig. 2) that was linked to the domination of *Stereocaulon alpinum* (see Electronic *Supplement Fig. S1)*. Diversity was low on younger plots due to substrate instability, and in older plots because of vascular plant competition (Asplund et al. 2022). This non-monotonic trend emphasizes the influence of gradient length: studies limited to shorter successional spans would likely overlook the late-stage declines captured within the 225-year gradient of this study.

Lichen cover and species composition form distinct zones along the successional gradient, reflecting a structured pattern of ecological replacement. A pronounced "*terricolous belt"* is observed in the intermediate stage, characterized by high coverage (~39%) of terricolous lichens – primarily *Stereocaulon. alpinum* and *Cladonia* spp. – and low saxicolous presence (Fig. 7b), what is in accordance with Nascimbene et al. (2017), who reported similar areas of terricolous lichen dominance for comparable moraine ages across several European glacier forefields. Flanking this central terricolous zone are two "saxicolous belts": a younger (~40–80 years) and an older (~100–160 years) stage, each dominated by saxicolous taxa such as *Lecidea promiscens*, *Lecanora polytropa*, and *Bellemerea* sp.. At both ends of the gradient (initial and oldest plots), lichen occurrence drops sharply, resulting in species-poor "edge communities" (Fig. 2 & 7).

These patterns are supported by multivariate ordinations. NMDS1 reflects a clear axis of substrate association, separating saxicolous and terricolous communities, while NMDS2 captures species richness gradients, with high values in intermediate stages and low values at the edges (Fig. 10). RDA similarly confirms community clustering along substrate and lichen cover gradients (Fig. 12). Plots within the saxicolous belts align with rock and saxicolous lichen coverage, whereas intermediate plots associate with soil and terricolous lichen cover. Edge plots show low diversity and align with high vegetation cover, which increases with successional age and acts as a proxy for community displacement (Nascimbene et al. 2017).

While most plots cluster distinctly, transitional stages are also present. Plot p042, though located within the younger saxicolous belt, exhibits high soil cover and substantial terricolous lichen presence – suggesting a lag in community turnover or transitional dynamics. Extensive investigations of several taxa in the same glacier forefield revealed a transition zone after ~60 years of deglaciation, where species turnover switches from stochastic occurrences towards deterministic processes such as niche filtering and biotic interactions (Hanusch et al. 2022). Aging ~55 years since deglaciation, p042 might reflect this transitional trend in community turnover.

## Symbiont interactions and assembly dynamics

The mycobiont–photobiont associations observed in this study are consistent with previously reported symbiotic partnerships, such as *Cladonia–Asterochloris* (Steinová et al. 2019), *Lecidea–Trebouxia* (Ruprecht et al. 2020), and *Porpidia–Asterochloris* (Ruprecht et al. 2016). Our network analysis reveals that the terricolous belt coincides with a photobiont guild dominated by *Asterochloris* species. This photobiont genus with 6 different species (Appendix Tab. A2) appears to act as an ecological filter, structuring which mycobionts can establish. For example, *Porpidia. macrocarpa* was the only lecideoid mycobiont present exclusively in these intermediate plots and was associated with a distinct *Asterochloris* lineage. The strong presence of *Asterochloris* in intermediate plots may relate to microclimatic conditions, particularly temperature (Peksa & Škaloud 2011), as the abundance of terricolous lichens correlated with mean annual temperature in the PCA (Fig. 11). *Asterochloris* photobionts may be more thermophilic compared to the more stress-tolerant *Trebouxia*, which is able to thrive under colder or nutrient-poor extremes, such as in polar studies (e.g. Wagner et al. 2020).

Next to microclimate regimes, the exceptionally high lichen coverage- and diversity on intermediate plots may further be facilitated by fine-grained, nutrient poor soils, which support terricolous lichens while limiting vascular plant encroachment. The dominating species, *Stereocaulon alpinum* is a tripartite lichen, possessing cyanobacterial photobionts next to green algae and it was hypothesized, that additional cyanobacteria symbionts enhance colonizing capability by binding N from the surrounding air what is advantageous on nutrient-poor substrates (Rikkinen 2015).

Older plots in contrast show distinctly higher nutrient levels, fostering vascular plant growth and likely increasing competitive pressure on lichens (Junker et al. 2020; Asplund et al. 2022). This combination of favourable substrate conditions and reduced competition appears to define a temporal ecological niche that supports lichen dominance during intermediate succession. The lichen flora may, in turn, modify microclimatic and soil conditions, facilitating a transition toward vascular plant dominance (Longton 1988).

Interestingly, the initial and late successional stages exhibit elevated network specialization, potentially due to environmental filtering effects. Both stages are clearly dominated by *Trebouxia* photobiont-guilds. In the initial stage, *Tr*_I01 is clearly the most dominant photobiont, which seems to be best adapted to low mean annual temperatures posed by the proximity to the glacier tongue. The late stage is dominated by *Tr*_S02, which is potentially adapted to higher temperatures.

Additionally, these two (initial and late) stages are marked by *Stereocaulon* species associating with OGEM-photobionts. This is in line with Vancurova et al. (2018), who report a wide ecological range of *Stereocaulon* species and the ability to associate with different photobionts of the genera *Asterochloris, Chloroidium* or *Vulcanochloris* Vancurová, Peksa, Nemcová & Skaloud. In the initial stage, *Stereocaulon nanodes* was exclusively associated to *Chloroidium saccharophilum*, while *S. alpinum* was associated to *Asterochloris* species throughout all other stages. This points towards *C. saccharophilum* might posing an advantage to *Stereocaulon* species for early colonization of ecologically challenging habitats, low temperatures, mobile substrate and limited nutrients (Barták et al. 2007; Türk & Erschbamer 2010; Wietrzyk-Pelka et al. 2018), likely being the most crucial environmental filters. In the late stage, *S. nanodes* associated to another OGEM algae, what possibly reflects a stress response due to vascular plant competition. The association of *Stereocaulon* species to microalgae like *C. saccharophilum* are rare (e.g. Beck 2002, Persoh et al. 2004, Ruprecht et al. 2014) and future studies should investigate the role of these exceptional symbiotic relations regarding assembly patterns and stress response (Vancurova et al. 2018).

## Field-assessable groupings and successional signals

Field-accessible groups based on morphological traits proved effective in capturing successional dynamics, supporting the value of trait-based lichen ecology (Ellis et al. 2021). *S. alpinum* served as a key indicator of intermediate-aged plots within the terricolous belt, while *Rhizocarpon* spp. dominated older saxicolous belts and showed strong correlations between thallus area and terrain age. *Cladonia* species were most diverse in the terricolous belt, with 'cladonia_s' showing a narrower distribution than the more widespread 'cladonia_r'. In contrast, species of *Aspicilia* and *Umbilicaria* were mostly restricted to early or late

successional stages. Core saxicolous groups such as 'lecanora', 'bellemerea', and 'lecideaceae' dominated mature rock-dominated communities. *Porpidia macrocarpa*, although grouped within 'lecideaceae', was restricted to mainly terricolous plots and may warrant a separate group. Yet, these groupings – based on field-visible characters – may offer a practical framework for interpreting successional patterns (Nascimbene et al. 2017), even in the absence of molecular data or advanced taxonomic tools.

### *Rhizocarpon* mean thallus area as proxy for succession?

Lichenometric approaches commonly estimate moraine age based on the diameter of the largest thalli of yellow *Rhizocarpon* species (e.g. Mottershead & White 1972; Proctor 1983; Garibotti & Villalba 2009). Statistical approaches (e.g. Loso et al. 2014) have also been developed that rely primarily on thalli from the upper part of the size distribution. However, exceptionally large individuals may represent coalesced thalli or may have been gravitationally transported from upslope areas, which can introduce uncertainty into size-based age estimates (Osborn et al. 2015). Rather, than focusing on the largest thalli, this pilot assessment explored whether outlier-corrected mean thallus area of yellow *Rhizocarpon* specimens may also reflect successional development. Significant relationships were found with both deglaciation age and total saxicolous lichen cover. Although these results suggest that population-level metrics may capture successional trends, a direct comparison with traditional diameter-based lichenometric approaches would be required to evaluate whether mean thallus area provides a methodological advantage. Such comparisons may represent a promising direction for future studies.

## Conclusion

This study presents one of the few molecular investigations of myco-/photobiont associations along a gradient in a glacier forefield (Beck et al. 2019), revealing distinct lichen communities well represented by field-assessable groups. Several of these groups serve as indicators of successional stage (Nascimbene et al. 2017) and environmental conditions. Photobiont-mediated guilds appear to structure mycobiont diversity along the successional gradient, and some associations – particularly the photobiont associations of *Stereocaulon* sp. (Vancurova et al. 2018) – are relevant and merit further study.

Standardized plots of Junker et al. (2020) enabled integration with abiotic and biotic datasets. Top-view imagery proved valuable for coverage assessment and for exploring an alternative age-dating method via outlier-corrected mean thallus area of yellow *Rhizocarpon*. This approach shows promise for broader application with expanded sampling and automated image analysis.

Overall, this pilot study advances understanding of lichen symbiont assembly in glacier forefields and highlights promising directions in molecular, and image-assisted research.

## Acknowledgements

We thank Roman Türk for his inexhaustible lichenological motivation, spirit and knowledge – his assistance during the fieldwork was highly appreciated. We are highly indebted

to Robert Junker for fruitful advice for the work on the Ödenwinkel Research Platform. Anna Götz brought forward this study by kindly sharing her knowledge and skills in molecular methods and data analyses. Thanks to Mareike Mittag for co-working, comments and discussions. We would also like to thank Wolf Ruetz for his language editing. We further thank the Nationalpark Hohe Tauern for the permission to conduct this study in the protected area (permit no. for the collection on 12.09.2022: 20507-96/77/9-2022).

This study was supported by the Funding Scholarship of the University of Salzburg and the molecular analyses was financially supported in part by the Austrian Sciences Fund (FWF) 10.55776/P35512.

## Electronic supplement

**S1:** Rectified top-view images of the plots chosen for this study (marked according to plot number). | **S1:** Rektifizierte Bilder aus der Vogelperspektive der für diese Studie ausgewählten Parzellen (gekennzeichnet nach Parzellennummer).

https://www.zobodat.at/pdf/supp/Gindorf_Rupprecht_Supplement_1.png

**S2:** Phylogeny of *Lecidea* and *Porpidia* based on ITS sequences (Ruprecht et al. 2020) and accessions of this study. Bootstrap values indicate branch support (≥90 = high). Coloured boxes highlight species clusters including accessions from this study. | **S2:** Phylogenie von *Lecidea* und *Porpidia* basierend auf ITS-Sequenzen (Ruprecht et al. 2020) und Proben aus dieser Studie. Die Bootstrap-Werte geben die Verzweigungsstärke an (≥90 = hoch). Die farbigen Kästchen heben Artencluster hervor, welche Proben aus der vorliegenden Studie enthalten.

https://www.zobodat.at/pdf/supp/Gindorf_Rupprecht_Supplement_2.png

**S3:** This phylogenetic overview shows the best sequence matches of the samples from this study obtained from BLAST search across a wide range of genera. Species that could not be directly assigned were classified only at the genus level. | **S3:** Dieser phylogenetische Überblick zeigt die besten Übereinstimmungen der Proben aus dieser Studie, die durch eine BLAST-Suche über ein breites Spektrum von Gattungen ermittelt wurden. Arten, die nicht direkt zugeordnet werden konnten, wurden lediglich auf Gattungsebene klassifiziert.

https://www.zobodat.at/pdf/supp/Gindorf_Rupprecht_Supplement_3.png

**S4:** Phylogeny of Trebouxia based on ITS sequences from Ruprecht et al. (2020) and this study. Bootstrap values (0–100) indicate branch support (≥90 = high). Coloured boxes highlight species clusters including accessions from this study. | **S4:** Phylogenie von Trebouxia basierend auf ITS-Sequenzen (Ruprecht et al. 2020) und Proben aus dieser Studie. Die Bootstrap-Werte geben die Verzweigungsstärke an (≥90 = hoch). Die farbigen Kästchen heben Artencluster hervor, welche Proben aus der vorliegenden Studie enthalten.

https://www.zobodat.at/pdf/supp/Gindorf_Rupprecht_Supplement_4.png

## References

Armstrong RA (2016) Lichenometric dating (Lichenometry) and the biology of the lichen genus Rhizocarpon: Challenges and future directions. Geografiska Annaler Series A 98, 183–206 (https://doi.org/10.1111/geoa.12130)

Asplund J, van Zuijlen K, Roos RE, Birkemoe T, Klanderud K, Lang SI, Wardle DA (2022) Divergent responses of functional diversity to an elevational gradient for vascular plants, bryophytes and lichens. Journal of Vegetation Science 33(1) (https://doi.org/10.1111/jvs.13105)

Barták M, Váczi P, Hájek J, Smykla J (2007) Low-temperature limitation of primary photosynthetic processes in Antarctic lichens *Umbilicaria antarctica* and *Xanthoria elegans*. Polar Biology 31(1), 47–51 (https://doi.org/10.1007/s00300-007-0331-x)

Beck A (2002) Selektivität der symbionten schwermetalltoleranter Flechten. München (ISBN: 3–9808102–0-8:1-200)

Beck A, Bechteler J, Casanova-Katny A, Dzhilyanova I (2019) The pioneer lichen *Placopsis* in maritime Antarctica: Genetic diversity of their mycobionts and green algal symbionts, and their correlation with deglaciation time. Symbiosis 79(1), 1–24 (https://doi.org/10.1007/s13199-019-00624-4)

Beck A, Casanova-Katny A, Gerasimova JV (2023) Metabarcoding of Antarctic lichens from areas with different deglaciation times reveals a high diversity of lichen-associated communities. Genes 14 (5), 1019 (https://doi.org/10.3390/genes14051019)

Bickford D, Lohman DJ, Sodhi NS, Ng PK, Meier R, Winker K, Ingram KK, Das I (2007) Cryptic species as a window on diversity and conservation. Trends in ecology & evolution 22(3), 148–155 (https://doi.org/10.1016/j.tree.2006.11.004)

Blaha J, Baloch E, Grube M (2006) High photobiont diversity associated with the euryoecious lichen-forming ascomycete *Lecanora rupicola* (Lecanoraceae, Ascomycota). Biological Journal of the Linnean Society 88(2), 283–293 (https://doi.org/10.1111/j.1095-8312.2006.00640.x)

Bradley JA, Singarayer JS, Anesio AM (2014) Microbial community dynamics in the forefield of glaciers. Proceedings of the Royal Society B: Biological Sciences 281(1795), 20140882 (https://doi.org/10.1098/rspb.2014.0882)

Büdel B, Colesie C (2014) Biological soil crusts. In: Cowan DA (2014) Antarctic terrestrial microbiology: Physical and biological properties of Antarctic soils. Springer 131–161 (https://doi.org/10.1007/978-3-642-45213-0_8)

Cannone N, Diolaiuti G, Guglielmin M, Smiraglia C (2008) Accelerating climate change impacts on alpine glacier forefield ecosystems in the European Alps. Ecological Applications 18(3), 637–648 (https://doi.org/10.1890/07-1188.1)

Dal Grande F, Rolshausen G, Divakar PK, Crespo A, Otte J, Schleuning M, Schmitt I (2018) Environment and host identity structure communities of green algal symbionts in lichens. New Phytologist 217(1), 277–289 (https://doi.org/10.1111/nph.14770)

Duran-Nebreda S, Valverde S (2022) Composition, structure and robustness of Lichen guilds. bioRxiv, 2022.2010.2030.514411 (https://doi.org/10.1101/2022.10.30.514411)

Ellis CJ, Asplund J, Benesperi R, Branquinho C, Di Nuzzo L, Hurtado P, Martinez I, Matos P, Nascimbene J, Pinho P, Prieto M, Rocha B, Rodriguez-Arribas C, Thus H, Giordani P (2021) Functional Traits in Lichen Ecology: A Review of Challenge and Opportunity. Microorganisms 9(4), (https://doi.org/10.3390/microorganisms9040766)

Erschbamer B, Caccianiga MS (2016) Glacier forelands: Lessons of plant population and community development. Progress in Botany Vol. 78, 259–284 (https://doi.org/10.1007/124_2016_4)

Faegri K (1934) Über die Längenvariationen einiger Gletscher des Jostedalsbre und die dadurch bedingten Pflanzensukzessionen. Bergens Museums Årbok 1933(2): 5–255

Favero-Longo SE, Worland MR, Convey P, Smith RIL, Piervittori R, Guglielmin M, Cannone N (2012) Primary succession of lichen and bryophyte communities following glacial recession on Signy Island, South Orkney Islands, Maritime Antarctic. Antarctic Science 24(4), 323–336 (https://doi.org/10.1017/s0954102012000120)

Gardes M, Bruns TD (1993) ITS primers with enhanced specificity for basidiomycetes-application to the identification of mycorrhizae and rusts. Molecular Ecology 2(2), 113–118 (https://doi.org/10.1111/j.1365-294x.1993.tb00005.x)

Garibotti IA, Villalba R (2009) Lichenometric dating using *Rhizocarpon* subgenus *Rhizocarpon* in the Patagonian Andes, Argentina. Quaternary research 71(3), 271–283 (https://doi.org/10.1016/j.yqres.2009.01.012)

Hanusch M, He X, Ruiz-Hernández V, Junker RR (2022) Succession comprises a sequence of threshold-induced community assembly processes towards multidiversity. Communications Biology 5(1), 424 (https://doi.org/10.1038/s42003-022-03372-2)

He X, Hanusch M, Ruiz-Hernández V, Junker RR (2023) Accuracy of mutual predictions of plant and microbial communities vary along a successional gradient in an alpine glacier forefield. Frontiers in Plant Science 13, 1017847 (https://doi.org/10.3389/fpls.2022.1017847)

Hoang DT, Chernomor O, Von Haeseler A, Minh BQ, Vinh LS (2018) UFBoot2: improving the ultrafast bootstrap approximation. Molecular biology and evolution 35(2), 518–522 (https://doi.org/10.1093/molbev/msx281)

Junker RR, Hanusch M, He X, Ruiz-Hernández V, Otto J-C, Kraushaar S, Bauch K, Griessenberger F, Ohler L-M, Trutschnig W (2020) Ödenwinkel: an Alpine platform for observational and experimental research on the emergence of multidiversity and ecosystem complexity. Web Ecology 20(2), 95–106 (https://doi.org/10.5194/we-20-95-2020)

Junker RR, He X, Otto J-C, Ruiz-Hernández V, Hanusch M (2021) Divergent assembly processes? A comparison of the plant and soil microbiome with plant communities in a glacier forefield. FEMS Microbiology Ecology 97(10), fiab135 (https://doi.org/10.1093/femsec/fiab135)

Kalyaanamoorthy S, Minh BQ, Wong TK, Von Haeseler A, Jermiin LS (2017) ModelFinder: fast model selection for accurate phylogenetic estimates. Nature methods 14(6), 587–589 (https://doi.org/10.1038/nmeth.4285)

Katoh K, Misawa K, Kuma K, Miyata T (2002) MAFFT: a novel method for rapid multiple sequence alignment based on fast Fourier transform. Nucleic acids research 30(14), 3059–3066 (https://doi.org/10.1093/nar/gkf436)

Kraichak E, Lücking R, Aptroot A, Beck A, Dornes P, John V, Lendemer JC, Nelsen MP, Neuwirth G, Nutakki A (2015) Hidden diversity in the morphologically variable script lichen (Graphis scripta) complex (Ascomycota, Ostropales, Graphidaceae). Organisms Diversity & Evolution 15(3), 447–458 (https://doi.org/10.1007/s13127-015-0219-5)

Kroken S, Taylor JW (2000) Phylogenetic species, reproductive mode, and specificity of the green alga *Trebouxia* forming lichens with the fungal genus *Letharia*. Bryologist 103(4), 645–660 (https://doi.org/10.1639/0007-2745(2000)103[0645:psrmas]2.0.co;2)

Longton RE (1988) Biology of polar bryophytes and lichens. Cambridge University Press 400 pp. (ISBN: 0521250153)

Loso MG, Doak DF, Anderson RS (2014) Licheno metric dating of Little Ice Age glacier moraines using explicit demographic models of lichen colonization, growth, and survival. Geografiska Annaler (Series A) 96, 21–41 (https://doi.org/10.1111/geoa.12022)

Lovell RS, Collins S, Martin SH, Pigot AL, Phillimore AB (2023) Space-for-time substitutions in climate change ecology and evolution. Biological Reviews 98(6), 2243–2270 (https://doi.org/10.32942/x2k018)

Lumbsch HT, Leavitt SD (2011) Goodbye morphology? A paradigm shift in the delimitation of species in lichenized fungi. Fungal Diversity 50(1), 59–72 (https://doi.org/10.1007/s13225-011-0123-z)

Miller HR, Lane SN (2019) Biogeomorphic feedbacks and the ecosystem engineering of recently deglaciated terrain. Progress in Physical Geography: Earth and Environment 43(1), 24–45 (https://doi.org/10.1177/0309133318816536)

Mottershead DM, White ID (1972) The lichenometric dating of glacier recession, Tunsbergdalsbre, Southern Norway. Geografiska Annaler (Series A) 54, 47–52 (https://doi.org/10.1080/04353676.1972.11879856)

Muggia L, Leavitt S, Barreno E (2018) The hidden diversity of lichenised Trebouxiophyceae (Chlorophyta). Phycologia 57(5), 503–524 (https://doi.org/10.2216/17-134.1)

Muggia L, Nelsen MP, Kirika PM, Barreno E, Beck A, Lindgren H, Lumbsch HT, Leavitt SD, Fernandez-Mendoza F, Perez-Ortega S, Grube M, Moya P, Molins A, Sadowska-Des A, Guzow-Krzeminska B, Ruprecht U, Dal Grande F, Singh G, Voytsekhovich A, Trebouxia Working G (2020) Formally described species woefully underrepresent phylogenetic diversity in the common lichen photobiont genus *Trebouxia* (Trebouxiophyceae, Chlorophyta): An impetus for developing an integrated taxonomy. Molecular Phylogenetics and Evolution 149 (https://doi.org/10.1016/j.ympev.2020.106821)

Nascimbene J, Mayrhofer H, Dainese M, Bilovitz PO (2017) Assembly patterns of soil-dwelling lichens after glacier retreat in the European Alps. Journal of Biogeography 44(6), 1393–1404 (https://doi.org/10.1111/jbi.12970)

Nelsen MP, Gargas A (2009) Symbiont flexibility in Thamnolia vermicularis (Pertusariales: Icmadophilaceae). Bryologist 112(2), 404–417 (https://doi.org/10.1639/0007-2745-112.2.404)

Nguyen L-T, Schmidt HA, Von Haeseler A, Minh BQ (2015) IQ-TREE: a fast and effective stochastic algorithm for estimating maximum-likelihood phylogenies. Molecular biology and evolution 32(1), 268–274 (https://doi.org/10.1093/molbev/msu300)

O'Brien J (2019) gdalUtilities: Wrappers for 'GDAL' Utilities Executables. (https://doi.org/10.32614/cran.package.gdalutilities)

Oksanen J, Blanchet FG, Kindt R, Legendre P, Minchin PR, O'hara R, Simpson GL, Solymos P, Stevens MHH, Wagner H (2013) Package 'vegan'. Community ecology package, version 2(9), 1–295 (https://doi.org/10.32614/cran.package.vegan)

Osborn G, McCarthy D, LaBrie A, Burke R (2015) Lichenometric dating: science or pseudo-science? Quaternary Research 83(1), 1–12 (https://doi.org/10.1016/j.yqres.2014.09.006)

Peay KG (2016) The mutualistic niche: mycorrhizal symbiosis and community dynamics. Annual Review of Ecology, Evolution, and Systematics 47(1), 143–164 (https://doi.org/annurev-ecolsys-121415-032100)

Peksa O, Škaloud P (2011) Do photobionts influence the ecology of lichens? A case study of environmental preferences in symbiotic green alga Asterochloris (Trebouxiophyceae). Molecular Ecology 20(18), 3936–3948 (https://doi.org/10.1111/j.1365-294x.2011.05168.x)

Perez-Ortega S, Ortiz-Álvarez R, Allan Green T, de Los Ríos A (2012) Lichen myco-and photobiont diversity and their relationships at the edge of life (McMurdo Dry Valleys, Antarctica). FEMS Microbiology Ecology 82(2), 429–448 (https://doi.org/10.1111/j.1574-6941.2012.01422.x)

Persoh D, Beck A, Rambold G (2004) The distribution of ascus types and photobiontal selection in Lecanoromycetes (Ascomycota) against the background of a revised SSU nrDNA phylogeny. Mycological Progress 3(2), 103–121 (https://doi.org/10.1007/s11557-006-0081-0)

Piercey-Normore MD, DePriest PT (2001) Algal switching among lichen symbioses. American journal of botany 88(8), 1490–1498 (https://doi.org/10.2307/3558457)

Proctor MCF (1983) Sizes and growth-rates of thalli of the lichen Rhizocarpon geographicum on the moraines of the Glacier de Valsorey, Valais, Switzerland. Lichenologist 15, 249–261 (https://doi.org/10.1017/S0024282983000389)

R Core Team. (2022) R: A Language and Environment for Statistical Computing. R Foundation for Statistical Computing, Vienna, Austria. (https://www.R-project.org/)

Rambaut A. (2018) FigTree: tree figure drawing tool, version 1.4.4. (https://www.tree.bio.ed.ac.uk)

Rikkinen J (2007) Photobiont-mediated lichen guilds. Comparative Biochemistry and Physiology Part A: Molecular & Integrative Physiology 146(4), S219–S220 (https://doi.org/10.1016/j.cbpa.2007.01.480)

Rikkinen J (2015) Cyanolichens. Biodiversity and conservation 24(4), 973–993 (https://doi.org/10.1007/s10531-015-0906-8)

Roe GH, Baker MB, Herla F (2017) Centennial glacier retreat as categorical evidence of regional climate change. Nature Geoscience 10(2), 95–99 (https://doi.org/doi.org/10.1038/ngeo2863)

Rolshausen G, Dal Grande F, Otte J, Schmitt I (2023) Lichen holobionts show compositional structure along elevation. Molecular Ecology 32(23), 6619–6630 (https://doi.org/10.1111/mec.16471)

Rolshausen G, Hallman U, Grande FD, Otte J, Knudsen K, Schmitt I (2020) Expanding the mutualistic niche: parallel symbiont turnover along climatic gradients. Proceedings of the Royal Society B 287(1924), 20192311 (https://doi.org/10.1098/rspb.2019.2311)

Ruprecht U, Brunauer G, Türk R (2014) High photobiont diversity in the common European soil crust lichen *Psora decipiens*. Biodiversity and conservation 23(7), 1771–1785 (https://doi.org/10.1007/s10531-014-0662-1)

Ruprecht U, Fernández-Mendoza F, Türk R, Fryday AM (2020) High levels of endemism and local differentiation in the fungal and algal symbionts of saxicolous lecideoid lichens along a latitudinal gradient in southern South America. The Lichenologist 52(4), 287–303 (https://doi.org/10.1017/s0024282920000225)

Ruprecht U, Lumbsch HT, Brunauer G, Green TGA, Turk R (2010) Diversity of *Lecidea* (Lecideaceae, Ascomycota) species revealed by molecular data and morphological characters. Antarctic Science 22(6), 727–741 (https://doi.org/10.1017/s0954102010000477)

Ruprecht U, Sochting U, Turk R (2016) *Porpidia navarina*, a new endemic species from Isla Navarino (southern Tierra del Fuego, Chile). Herzogia 29(2), 596–609 (https://doi.org/10.13158/heia.29.2.2016.596)

Sanders WB, Masumoto H (2021) Lichen algae: the photosynthetic partners in lichen symbioses. The Lichenologist 53(5), 347–393 (https://doi.org/10.1017/s0024282921000335)

Schumann K, Gewolf S, Tackenberg O (2016) Factors affecting primary succession of glacier foreland vegetation in the European Alps. Alpine Botany 126(2), 105–117 (https://doi.org/10.1007/s00035-016-0166-6)

Steinova J, Skaloud P, Yahr R, Bestova H, Muggia L (2019) Reproductive and dispersal strategies shape the diversity of mycobiont-photobiont association in Cladonia lichens. Molecular Phylogenetics and Evolution, 134, 226–237 (https://doi.org/10.1016/j.ympev.2019.02.014)

Türk R, Erschbamer B (2010) Die Flechten im Gletschervorfeld des Rotmoosferners. In: Koch E-M, Erschbamer B (2010) Glaziale und periglaziale Lebensräume im Raum Obergurgl. Alpine Forschungsstelle Obergurgl 1, Innsbruck University Press, Innsbruck 155–164 (https://doi.org/10.26530/OAPEN_459081)

Vancurova L, Muggia L, Peksa O, Ridka T, Skaloud P (2018) The complexity of symbiotic interactions influences the ecological amplitude of the host: A case study in *Stereocaulon* (lichenized Ascomycota). Molecular Ecology 27(14), 3016–3033 (https://doi.org/10.1111/mec.14764)

Wagner M, Bathke AC, Cary SC, Green TGA, Junker RR, Trutschnig W, Ruprecht U (2020) Myco- and photobiont associations in crustose lichens in the McMurdo Dry Valleys (Antarctica) reveal high differentiation along an elevational gradient. Polar Biology 43(12), 1967–1983 (https://doi.org/10.1007/s00300-020-02754-8)

Wagner M, Brunauer G, Bathke AC, Cary SC, Fuchs R, Sancho LG, Türk R, Ruprecht U (2021) Macroclimatic conditions as main drivers for symbiotic association patterns in lecideoid lichens along the Transantarctic Mountains, Ross Sea region, Antarctica. Scientific Reports 11(1), 23460 (https://doi.org/10.1038/s41598-021-02940-6)

Warnes MGR, Bolker B, Bonebakker L, Gentleman R, Huber W (2016) Package 'gplots'. Various R programming tools for plotting data, (https://doi.org/10.32614/cran.package.gplots)

White TJ, Bruns T, Lee S, Taylor J (1990) Amplification and direct sequencing of fungal ribosomal RNA genes for phylogenetics. In Innis MA, Gelfand DH, Sninsky JJ, White TJ (1989) PCR protocols: a guide to methods and applications. Academic Press 315–322 (https://doi.org/10.1016/b978-0-12-372180-8.50042-1)

Wickham H, Hester J, Chang W, Bryan J (2022) devtools: Tools to Make Developing R Packages Easier (https://doi.org/10.32614/cran.package.devtools)

Wietrzyk-Pelka P, Otte V, Wegrzyn MH, Olech M (2018) From barren substrate to mature tundra-lichen colonization in the forelands of Svalbard glaciers. Acta Societatis Botanicorum Poloniae 87(4) (https://doi.org/10.5586/asbp.3599)

Yahr R, Schoch CL, Dentinger BTM (2016) Scaling up discovery of hidden diversity in fungi: impacts of barcoding approaches. Philosophical Transactions of the Royal Society B-Biological Sciences 371(1702) (https://doi.org/10.1098/rstb.2015.0336)

Zavarzina AG, Nikolaeva TN, Demin VV, Lapshin PV, Makarov MI, Zavarzin AA, Zagoskina NV (2019) Water-soluble phenolic metabolites in lichens and their potential role in soil organic matter formation at the pre-vascular stage. European Journal of Soil Science 70(4), 736–750 (https://doi.org/10.1111/ejss.12822)

# Appendix

**Tab. A1:** Year of deglaciation, elevation and coordinates for the eleven plots of Research Platform Ödenwinkel (Junker et al. 2020) chosen for this study. | **Tab. A1:** Jahr der Entgletscherung, Höhe und Koordinaten der elf für diese Studie ausgewählten Parzellen der Forschungsplattform Ödenwinkel (Junker et al. 2020).

| Plot Number | Year of deglaciation (YD) | Age (2022 – YD) | Elevation [m asl] | Longitude | Latitude |
|---|---|---|---|---|---|
| p004 | 2008 | 14 | 2165.9 | 12.63944 | 47.12106 |
| p010 | 1985 | 37 | 2159.9 | 12.63916 | 47.12163 |
| p030 | 1976 | 46 | 2142.1 | 12.63843 | 47.12382 |
| p042 | 1967 | 55 | 2133.1 | 12.63793 | 47.12481 |
| p055 | 1955 | 67 | 2122.2 | 12.6368 | 47.12569 |
| p073 | 1939 | 83 | 2110.3 | 12.63519 | 47.12712 |
| p089 | 1924 | 98 | 2102.4 | 12.63406 | 47.12788 |
| p101 | 1909 | 113 | 2100.1 | 12.63366 | 47.12856 |
| p120 | 1882 | 140 | 2085.9 | 12.63384 | 47.12964 |
| p126 | 1869 | 153 | 2083.1 | 12.63403 | 47.13017 |
| p140 | 1797 | 225 | 2055.6 | 12.63776 | 47.13482 |

**Tab A2:** Full list of obtained species identities from molecular analyses of all samples collected in the field and accession numbers including published species names. OGEM refers to "Other Green Eucaryotic Microalgae". The "per ident" values from BLAST search were appended directly to the photobiont assignments for the single haplotypes. | **Tab A2:** Vollständige Liste der Arten basierend auf molekularen Analysen aller im Feld gesammelten Proben sowie der Zugangsnummern ("accession number") einschließlich der veröffentlichten Artnamen. OGEM steht für „Other Green Eucaryotic Microalgae" (andere grüne eukaryotische Mikroalgen). Die „per ident"-Werte aus der BLAST-Suche wurden direkt neben den Zuordnungen der Photobionten für die einzelnen Haplotypen angefügt.

| Plot | Voucher ID | Mycobiont | Trebouxia | Asterochloris | OGEM | Acc. Num. Mycobiont | Acc. Num. Photobiont |
|---|---|---|---|---|---|---|---|
| p004 | UR01414 | *Stereocaulon nanodes* | | | *Chloroidium saccharophilum/100* | PX023465 | PV990947 |
| p010 | UR01415 | *Lecidea* sp. | *Tr_* I01 | | | PX023420 | PV990905 |
| p010 | UR01416 | *Rhizocarpon* cf. *geographicum* | *Tr_* I01/ *98.70* | | | PX023405 | PV990910 |
| p010 | UR01417 | *Lecidea* sp. | *Tr_* S02/ *100* | | | PX023421 | PV990915 |
| p010 | UR01418 | *Lecidea* sp. | *Tr_* S02 | | | PX023422 | PV990915 |
| p030 | UR01419 | *Lecanora* cf. *polytropa* | *Tr_* I01 | | | PX023442 | PV990905 |
| p030 | UR01420 | *Lecidea promiscens* | *Tr_* I01 | | | PX023429 | PV990905 |
| p030 | UR01421 | *Bellemerea alpina* cf. *Bellemerea* sp. | *Tr_* S02 | | | PX023416 | PV990915 |
| p030 | UR01422 | *Bellemerea alpina* cf. *Bellemerea* sp. | *Tr_* S02 | | | PX023417 | PV990915 |
| p030 | UR01423 | *Umbilicaria aprina* *Umbilicaria* sp. | *Tr_* S02 | | | PX023453 | PV990915 |
| p030 | UR01424 | *Stereocaulon alpinum* *Stereocaulon nanodes* | | | *Chloroidium* cf. *saccharophilum/94.12* | PX023466 | PV990948 |
| p030 | UR01425 | *Lecidea* sp. | *Tr_* I01 | | | PX023431 | PV990905 |
| p030 | UR01426 | *Rhizocarpon* cf. *geographicum* | *Tr_* I01/ *99.85* | | | PX023401 | PV990907 |
| p030 | UR01427 | *Lecidea promiscens* | *Tr_* I01/ *99.69* | | | PX023432 | PV990908 |
| p030 | UR01428 | *Rhizocarpon* cf. *polycarpum* | *Tr_* I01 | | | PX023406 | PV990905 |
| p042 | UR01442 | *Cladonia coniocraea* *Cladonia pyxidata* | | *A. glomerata/100* | | PX023476 | PV990929 |
| p042 | UR01443 | | | *A.* sp. Vancourova A588/100 | | | PV990925 |

| Plot | Voucher ID | Mycobiont | Trebouxia | Asterochloris | OGEM | Acc. Num. Mycobiont | Acc. Num. Photobiont |
|---|---|---|---|---|---|---|---|
| p042 | UR01444 | *Lecidea promiscens* | *Tr_*I01/ *100* | | | PX023423 | PV990914 |
| p042 | UR01445 | *Lecanora* cf. *polytropa* | *Tr_*S02 | | | PX023446 | PV990915 |
| p042 | UR01446 | *Stereocaulon alpinum* | | *A.* sp. Vancourova A588/*99.79* | | PX023458 | PV990917 |
| p042 | UR01447 | *Rhizocarpon* cf. *geographicum* | *Tr_*I01 | | | PX023403 | PV990905 |
| p042 | UR01448 | *Lecidea promiscens* | *Tr_*I01 | | | PX023434 | PV990905 |
| p042 | UR01449 | *Lecidea promiscens* | *Tr_*I01 | *A. glomerata/100* | | PX023433 | PV990905 PV990933 |
| p042 | UR01450 | *Lecidea promiscens* | *Tr_*I01/ 98.70 | | | PX023424 | PV990913 |
| p042 | UR01451 | *Stereocaulon alpinum* | | *A.* sp. Vancourova A588/*99.79* | | PX023459 | PV990918 |
| p042 | UR01452 | *Rhizocarpon polycarpum* | *Tr_*S02 | | | PX023408 | PV990915 |
| p055 | UR01429 | *Cladonia macropyloides* | | *A. glomerata/ 99.81* | | PX023473 | PV990926 |
| p055 | UR01430 | *Cladonia macropyloides* | | *A. glomerata/100* | | PX023474 | PV990927 |
| p055 | UR01431 | *Lecidea promiscens* | | *A. glomerata/100* | | PX023433 | PV990922 |
| p055 | UR01432 | *Rhizocarpon* cf. *polycarpum* | *Tr_*I01 | *A. glomerata/100* | | PX023407 | PV990905 PV990928 |
| p055 | UR01433 | *Cladonia macrophyllodes Cladonia macropyloides* | | *A. glomerata/100* | | PX023475 | PV990935 |
| p055 | UR01434 | *Lecidea promiscens* | *Tr_*I01/ *99.69* | | | PX023427 | PV990909 |
| p055 | UR01435 | *Rhizocarpon* cf. *geographicum* | | | | PX023402 | |
| p055 | UR01436 | *Lecidea promiscens* | *Tr_*I01 | | | PX023428 | PV990905 |
| p055 | UR01437 | *Lecanora* cf. *polytropa* | *Tr_*I01 | | | PX023444 | PV990905 |
| p055 | UR01438 | *Bellemerea alpina* cf. *Bellemerea* sp. | *Tr_*I01/ *98.70* | | | PX023414 | PV990911 |
| p055 | UR01439 | *Lecanora* cf. *polytropa* | *Tr_*I01 | | | 1445 | PV990905 |
| p055 | UR01440 | *Aspicilia simoensis* | *Tr_*I01 | | | PX023456 | PV990905 |
| p055 | UR01441 | *Lecanora* cf. *polytropa* | | | | PX023443 | |

| Plot | Voucher ID | Mycobiont | Trebouxia | Asterochloris | OGEM | Acc. Num. Mycobiont | Acc. Num. Photobiont |
|---|---|---|---|---|---|---|---|
| p073 | UR01453 | | | *A. glomerata/100* | | | PV990936 |
| p073 | UR01454 | *Cladonia ecmocyna* | | *A. irregularis/ 100* | | PX023477 | PV990942 |
| p073 | UR01455 | *Stereocaulon alpinum* | | *A. lobophora/ 99.28* | | PX023461 | PV990921 |
| p073 | UR01456 | *Stereocaulon alpinum* | | *A.* sp. Vancourova A588/*99.79* | | PX023462 | PV990923 |
| p073 | UR01457 | *Porpidia macrocarpa* | | *A. stereo-caulonicola/100* | | PX023439 | PV990924 |
| p073 | UR01458 | *Lecidea promiscens* | | | | PX023425 | |
| p089 | UR01459 | *Porpidia macrocarpa* | | *A. glomerata/100* | | PX023440 | PV990937 |
| p089 | UR01460 | *Cetraria islandica* | *Tr_* S02 | | | PX023449 | PV990915 |
| p089 | UR01461 | *Cladonia ecmocyna* | | *A. irregularis/ 100* | | PX023478 | PV990938 |
| p089 | UR01462 | *Porpidia macrocarpa* | | *A. irregularis/ 100* | | PX023441 | PV990939 |
| p089 | UR01463 | *Cladonia macroceras* | | *A. glomerata/100* | | PX023480 | PV990931 |
| p089 | UR01464 | *Cetraria islandica* | | *A. glomerata/100* | | PX023450 | PV990930 |
| p089 | UR01465 | *Cladonia mitis* | | *A. irregularis/ 100* | | PX023471 | PV990940 |
| p089 | UR01466 | *Cladonia uncialis* susp. *uncialis* | | *A. glomerata/100* | | PX023469 | PV990943 |
| p089 | UR01467 | *Cladonia ecmocyna* | | *A. glomerata/100* | | PX023479 | PV990932 |
| p089 | UR01468 | *Stereocaulon alpinum* | | *A.* sp. Vancourova A588/*99.79* | | PX023460 | PV990919 |
| p089 | UR01469 | *Rhizocarpon* cf. *geographicum* | *Tr_* I01 | | | PX023404 | PV990905 |
| p089 | UR01470 | *Cladonia* cf. | | | | PX023481 | |
| p089 | UR01471 | *Cladonia squamosa* | | *A. irregularis/ 100* | | PX023472 | PV990941 |
| p101 | UR01403 | *Cladonia luteoalba* | | | | PX023467 | |
| p101 | UR01404 | cf. *Bellemerea* sp. | *Tr_* S02 | | | PX023415 | PV990915 |
| p101 | UR01405 | *Lecidea* sp. UR01405 | *Tr_* S02 | | | PX023435 | PV990915 |
| p101 | UR01406 | *Umbilicaria* sp | *Tr_* S02 | | | PX023452 | PV990915 |
| p101 | UR01407 | *Lecidea lapicida* | *Tr_* S02 | | | PX023436 | PV990915 |

| Plot | Voucher ID | Mycobiont | Trebouxia | Asterochloris | OGEM | Acc. Num. Mycobiont | Acc. Num. Photobiont |
|---|---|---|---|---|---|---|---|
| p101 | UR01408 | *Lecidea promiscens* | *Tr_* I01 | | | PX023426 | PV990905 |
| p101 | UR01409 | *Rhizocarpon* cf. *geographicum* | *Tr_* S02 | | | PX023399 | PV990915 |
| p101 | UR01410 | *Lecidea plana* | | | *Pseudochlorella pyrenoidosa/99.29* | PX023438 | PV990946 |
| p101 | UR01411 | *Lecanora* cf. *polytropa* | *Tr_* S02 | | | | PV990915 |
| p101 | UR01412 | *Stereocaulon nanodes* | | | Unknown algal isolate | PX023464 | PV990949 |
| p101 | UR01413 | | *Tr_* I01/ *99.71* | | | | PV990906 |
| p120 | UR01472 | *Rhizocarpon* cf. *geographicum* | *Tr_* S02 | | | PX023400 | PV990915 |
| p120 | UR01473 | *Umbilicaria* cf. *umbilicarioides* | *Tr_* S02 | | | PX023454 | PV990915 |
| p120 | UR01474 | *Cladonia sulphurina* | | *A. glomerata/100* | | PX023468 | PV990934 |
| p120 | UR01475 | *Lecidea promiscens* | *Tr_* I01/ 98.70 | | | PX023430 | PV990912 |
| p120 | UR01476 | | *Tr_* I01 | | | | PV990905 |
| p120 | UR01477 | | *Tr_* S02 | | | | PV990915 |
| p120 | UR01478 | cf. *Bellemerea* sp. | *Tr_* S02 | | | PX023418 | PV990915 |
| p120 | UR01479 | *Lecanora* cf. *polytropa* | *Tr_* S02 | | | PX023448 | PV990915 |
| p120 | UR01480 | *Rhizocarpon* cf. *polycarpum* | *Tr_* S02 | | | PX023409 | PV990915 |
| p120 | UR01481 | | *Tr_* S02 | | | | PV990915 |
| p120 | UR01482 | *Lecanora* cf. *polytropa* | *Tr_* S02 | | | PX023447 | PV990915 |
| p120 | UR01483 | *Stereocaulon alpinum* | | *A. lobophora/ 99.28* | | PX023463 | PV990920 |
| p120 | UR01484 | *Rhizocarpon* cf. *geographicum* | *Tr_* S02 | | | PX023398 | PV990915 |
| p126 | UR01394 | *Rhizocarpon* cf. *geographicum* | *Tr_* I01/ *99.86* | | | PX023396 | PV990905 |
| p126 | UR01395 | *Bellemerea* cf. *alpina* | *Tr_* I01 | | | PX023410 | PV990905 |
| p126 | UR01396 | *Lecidea* sp. | *Tr_* I01 | | | PX023419 | PV990905 |
| p126 | UR01397 | *Bellemerea* cf. *alpina* | *Tr_* I01 | | | PX023413 | PV990905 |
| p126 | UR01398 | *Bellemerea* cf. *alpina* | *Tr_* I01 | | | PX023411 | PV990905 |
| p126 | UR01399 | *Aspicilia zonata* | *Tr_* I01 | | | PX023455 | PV990905 |
| p126 | UR01400 | *Rhizocarpon* cf. *geographicum* | *Tr_* S02/ *100* | | | PX023397 | PV990915 |

| Plot | Voucher ID | Mycobiont | Trebouxia | Asterochloris | OGEM | Acc. Num. Mycobiont | Acc. Num. Photobiont |
|---|---|---|---|---|---|---|---|
| p126 | UR01401 | *Bellemerea* cf. *alpina* | *Tr_* I01 | | | PX023412 | PV990905 |
| p126 | UR01402 | *Stereocaulon alpinum* | | *A.* sp. *2709/99.46* | | PX023457 | PV990916 |
| p140 | UR01485 | *Cladonia arbuscula* | | *A. glomerata/100* | | | PV990944 |
| p140 | UR01486 | *Cetraria islandica* | | | | PX023451 | |
| p140 | UR01487 | *Cladonia rangiferina* | | *A. glomerata/100* | | PX023470 | PV990945 |